Copy No. 100

RESTRICTED

RM No. A7G03

NACA RM No. A7G03

RESEARCH MEMORANDUM

AN ANALYSIS OF LONGITUDINAL-CONTROL PROBLEMS ENCOUNTERED IN FLIGHT AT TRANSONIC SPEEDS WITH A JET-PROPELLED AIRPLANE

By

Harvey H. Brown, L. Stewart Rolls,
and Lawrence A. Clousing

Ames Aeronautical Laboratory
Moffett Field, Calif.

CLASSIFIED DOCUMENT

NATIONAL ADVISORY COMMITTEE
FOR AERONAUTICS

WASHINGTON

September 25, 1947

RESTRICTED

NACA RM No. A7G03

NATIONAL ADVISORY COMMITTEE FOR AERONAUTICS

RESEARCH MEMORANDUM

AN ANALYSIS OF LONGITUDINAL-CONTROL PROBLEMS ENCOUNTERED IN FLIGHT AT TRANSONIC SPEEDS WITH A JET-PROPELLED AIRPLANE

By Harvey H. Brown, L. Stewart Rolls,
and Lawrence A. Clousing

SUMMARY

During flight tests of a jet-propelled airplane, a sudden pitch-up motion of the airplane occurred in a recovery from a high-speed dive, although the pilot had not moved the controls so as to produce this motion. The pitch-up occurred at a Mach number of 0.85 as the Mach number was being decreased from 0.866 and resulted in a change of lift coefficient from 0.49 to 0.89 in about 1 second.

Measurements of the stability and control characteristics of the airplane and of the wing pressure distribution during the dive and recovery are presented.

An analysis based on flight and wind-tunnel data indicated the probable causes of the abrupt pitch-up were an abrupt restoration of elevator effectiveness and a nose-up change in balance caused by a shift in the angle of attack for zero lift both due to the decreasing Mach number.

INTRODUCTION

During flight tests of a jet-propelled airplane conducted for the purpose of obtaining high-speed aerodynamic characteristics, several problems of high-speed flight were encountered. Some of the data obtained and a discussion of the problems encountered were presented in reference 1 which dealt with wing-pressure measurements.

On one of the flights the airplane abruptly pitched up to the stall in about 1 second during a dive recovery. This abrupt

pitching-up motion was experienced at a Mach number of 0.85 as the Mach number of flight was being decreased from a value of 0.866, although the pilot had not moved the controls significantly. The airplane had not exhibited this trait in pull-outs up to the stall at lower Mach numbers.

Because preliminary analysis indicated that the action of the horizontal tail was responsible for the abrupt pitch-up, tests were made of a 1/3-scale model of the horizontal tail in the Ames 16-foot high-speed wind tunnel up to the Mach numbers attained in flight. Because it appeared that a swept tail would alleviate or eliminate the pitching-moment effects, wind-tunnel tests were also made of the tail with the quarter-chord line swept back 56.5°.

This report presents an analysis based on flight and wind-tunnel test data directed toward the determination of the probable cause of the abrupt pitch-up. Wing pressure distributions and stability and control characteristics in the dive are also included.

SYMBOLS

A_X	airplane longitudinal acceleration factor (X/W)
A_Z	airplane normal acceleration factor (Z/W)
a	horizontal distance from 0.25 M.A.C. to the airplane center of gravity, feet
b	wing span, feet
B	moment of inertia of airplane about its lateral axis, pound-feet, second squared
c	section chord, feet
$\bar{c}$	wing mean aerodynamic chord, feet
c_n	section normal-force coefficient $\left[\int_0^{1.0}(P_L-P_U)\,d\left(\frac{x}{c}\right)\right]$
$c_{m_{c/4}}$	section pitching-moment coefficient about quarter chord $\left[\int_0^{1.0}(P_U-P_L)\left(\frac{x}{c}-0.25\right)d\left(\frac{x}{c}\right)\right]$
C_X	airplane longitudinal-force coefficient $\left(\frac{WA_X}{qS}+\frac{T}{qS}\right)$

C_{L_H}	lift coefficient of horizontal tail
C_L	airplane lift coefficient
C_m	pitching-moment coefficient about airplane center of gravity
$C_{m_{fus}}$	pitching-moment coefficient of fuselage about the airplane center of gravity
C_{m_H}	horizontal-tail pitching-moment coefficient about the airplane center of gravity
$C_{m_{c/4}}$	pitching-moment coefficient of wing about 0.25 M.A.C.
C_N	airplane normal-force coefficient (WA_Z/qS) (C_N in this report is identical to the C_L usually used in flight-research results)
F_e	elevator-control force, pounds
g	acceleration due to gravity, 32.2 feet per second per second
H	total pressure, pounds per square foot
h_p	pressure altitude, feet
i_t	incidence angle of the horizontal tail, degrees
k	constant
l	tail length, feet
M	Mach number, ratio airspeed to speed of sound
P	pressure coefficient $[(p-p_o)/q]$
P_U	pressure coefficient on upper surface
P_L	pressure coefficient on lower surface
p	static orifice pressure, pounds per square foot
p_o	free-stream static pressure, pounds per square foot

p_{SL} standard barometric pressure at sea level, pounds per square foot

q dynamic pressure $(\frac{1}{2}\rho V^2)$, pounds per square foot

q_H dynamic pressure at horizontal tail, pounds per square foot

S wing area, square feet

S_H horizontal tail area, square feet

t section airfoil thickness, feet

T thrust, pounds

V airspeed, feet per second

V_i indicated airspeed, miles per hour

$$\left\{V_i = 1703\left[\left(\frac{H-p_o}{p_{SL}} + 1\right)^{0.286} - 1\right]^{\frac{1}{2}}\right\}$$

w downwash velocity aft of the wing center section, feet per second

W airplane gross weight, pounds

x chordwise distance from leading edge, feet

X aerodynamic longitudinal force on airplane, pounds

y spanwise distance from plane of symmetry, feet

Z aerodynamic normal force on airplane, pounds

z vertical distance from 0.25 M.A.C. to the airplane center of gravity, feet

α angle of attack of the airplane thrust line, degrees

α_H angle of attack of horizontal tail, degrees

ρ air density, slugs per cubic foot

δ_a aileron control-surface deflection, degrees

δ_e elevator control-surface deflection, degrees

Λ angle of sweepback of quarter-chord line, degrees

θ angle of airplane longitudinal axis with respect to axis fixed in space, radians

τ time, seconds

ϵ downwash angle, degrees

$d\theta/d\tau$ pitching angular velocity, radians per second

$d^2\theta/d\tau^2$ pitching angular acceleration, radians per second per second

DESCRIPTION OF THE AIRPLANE

The airplane used in the tests is shown in figures 1 and 2. Figure 3 is a three-view drawing of the airplane showing the wing stations at which pressure measurements were taken. Dimensions of the airplane wing and the horizontal tail are listed in table I. Table II contains the ordinates for the wing sections (NACA 65_1-213 (a=0.5)) and table III lists the orifice locations for the four stations on the left wing. The deviations of the actual contour from the theoretical contour are plotted in figure 4.

The plan form and contour of the horizontal stabilizer and elevator are shown in figure 5. The elevator was equipped with a trim tab which also acted as a boost tab with a 1:3 ratio and with a spring tab which operated when the pull forces on the stick exceeded approximately 10 pounds. The spring tab reached a maximum deflection of about 25° at about 50 pounds pull force.

The gross weight of the airplane during the dive was 10,220 pounds with the center of gravity at 27.5 percent of the mean aerodynamic chord.

Standard NACA recording instruments were used to record the various quantities during the flight. The wing orifice pressures were recorded simultaneously on multiple manometers housed in the fuselage nose compartment. A more complete description of the instrumentation is given in reference 1.

ACCURACY OF RESULTS

The static pressures used in the determination of the airspeed and altitude were obtained from the static pressure of the airspeed head corrected for position error as determined from a low-altitude flight calibration. The flight calibration was made by flying the airplane past an object of known height to obtain the pressure difference between the airplane static pressure and the barometric pressure. In addition, from a calibration made in the Ames 16-foot high-speed wind tunnel the error inherent in the airspeed head due to compressibility was determined. The values of pressure coefficients were based on corrected static pressures.

All pressure lines of the airspeed system were balanced to provide equal rates of flow during rapid changes in altitude. In order to avoid the use of an excessively long impact pressure line to provide equal rates of flow, two separate sources of static pressure were provided, one for the airspeed recorder and one for the altitude recorder. All lines were 3/16-inch inside diameter and about 7 feet long, for which length the lag was considered negligible.

The airspeed instrument, altimeter, and all pressure cells were calibrated at several temperatures and the flight-test data were corrected for instrument temperature effects.

Due to the high angles of attack and high Mach numbers obtained during the dive, the calibration of the airspeed system had to be necessarily extrapolated to a considerable extent. For the portion of the dive between $\tau = 13.0$ and 15.0 (fig. 6), the accuracy is less than for the rest of the dive, and therefore two sets of values of accuracy are given.

Time Interval	6.0 – 13.0 sec., 15.0 – 18.0 sec.	13.0 – 15.0 sec.
V_i	±0.7 mph	±2 mph
M	±0.005	±0.015
h_p	±50 feet	±200 feet
P	±10/q	(noted)

The values of aileron angle shown in figure 6 are for the right aileron. It was assumed that the left aileron was at the same angle. During the pull-out some aileron force was applied so there is an indeterminate error in the aileron position.

Due to instrumentation difficulties no reliable records of the elevator trim tab or spring-tab deflections were obtained during the flight. The deflection of the trim (boost) tab varied less than 5° for the elevator deflections obtained but the spring tab was most likely at full deflection (25°) during the pull-out when the control forces were high. In view of the uncertainty of the tab deflections, their effect has been ignored in the analysis. The effect of the tabs was to cause a higher value of up-elevator deflection than would have occurred had the tabs been at zero deflection. This difference in elevator angle during the dive varies from about zero at zero value of C_N to about 2° at values of C_N above 0.5.

The pressure cell which recorded the difference in static pressure between the nose compartment and the airspeed head gave incorrect results at the higher values of C_L and therefore the pressure coefficients were uncorrected and are noted as such where presented.

During the abrupt pitch-up portion of the dive many of the orifice pressures changed very rapidly and for this reason no estimate is made of the accuracy of P for this period.

RESULTS AND DISCUSSION

A time history of various quantities measured during the dive recovery is shown in figure 6. From a maximum dive angle of about 40° a gradually increasing rate of recovery was carried out up to 13.3 seconds. The airplane normal-force coefficient at this time was approximately 0.49 at a Mach number of 0.858. At this point, without appreciable change in elevator angle, the airplane suddenly pitched up to $C_N = 0.89$ at $M = 0.844$ during a time interval of about 1 second. The maximum C_N occurred at about 14.25 seconds with the maximum angle of attack indicated as occurring slightly later, which suggested that a stall had been encountered and which was later verified from the pressure-distribution measurements.

The maximum Mach number, 0.866, was reached at about 11.75 seconds. As the pull-out progressed the Mach number decreased, the rate of decrease being very rapid near the end of the pull-out.

The chordwise pressure distributions obtained during the pull-out are presented in figure 7. Comparison of the pressure distribution for wing station 65 in figure 7(h) ($\tau = 14.25$) and figure 7(i) ($\tau = 14.45$) shows the flat distribution on the upper surface indicative of a stalled condition. This stall was apparently confined to the center section.

The spanwise loadings derived from these chordwise pressure distributions are presented in figure 8. In considering these data it should be noted that the ailerons were floating up as indicated in figure 7.

The variation of elevator angle with Mach number for constant values of airplane normal-force coefficient is shown in figure 9. The values below $M = 0.80$ were obtained from straight flight runs and shallow turns. The results for the higher Mach numbers were obtained from dive pull-outs at $M = 0.82$ to 0.83 and from the dive for which the time history is shown in figure 6.

Inasmuch as the angular pitching velocity of the airplane during a pull-out produces an increase in the angle of attack of the tail over that obtained in level flight, an increase in up-elevator deflection is necessary to offset this effect. In figure 9 the elevator angles obtained from pull-outs have been reduced to the static case by employing the horizontal-tail characteristics determined from tests on a 1/3-scale model of the complete airplane in the Ames 16-foot high-speed wind tunnel (reference 2). These wind-tunnel results are shown in figure 10. The elevator angles obtained during the pitch-up were further reduced to correct for the out-of-balance attitude of the airplane.

The calculated longitudinal-stability curves of figure 11 were obtained from the elevator-deflection values of figure 9, utilizing the elevator effectiveness of figure 10. This is an apparent static longitudinal stability since the elevator effectiveness, as will be seen later, may differ from that shown in figure 10.

The various longitudinal stability and balance problems encountered in the high-speed dives and recoveries of this airplane are indicated in figures 9 and 11. The problems indicated in figure 9 are (1) an increase in up-elevator angle required for balance or a nose-down tendency at Mach numbers greater than 0.70; (2) a further increase in elevator angle required for balance for values of C_N above 0.20 at Mach numbers above 0.75 as shown by the spreading apart of the curves for $C_N = 0.2$ and $C_N = 0.4$; and (3) the abrupt decrease in elevator angles required for balance at the higher normal-force coefficients at $M = 0.84$ to 0.86, indicated by the bending over of the curves for the higher lift coefficients.

Nose-Down Tendency

The airplane nose-down tendency (problem (1)) was encountered in wind-tunnel tests (reference 2) as well as in flight. The increment in elevator angle needed to balance this pitching moment above $M = 0.70$ at $C_N = 0$ is presented in figure 12(a) for both wind-tunnel tests and flight. The change occurs more abruptly and at a higher Mach number in the case of the wind-tunnel tests than for the flight tests. This less abrupt change in flight is possibly due to the action of the spring tab. However, it was considered reasonable to attribute the change in balance in both cases to the same cause and therefore conclusions drawn from analyses of the wind-tunnel results could be applied to flight-test results.

The angle of attack for zero lift for the airplane model in the wind-tunnel is presented in figure 12(b). For a constant value of C_N and assuming ϵ to be solely a function of C_N, then a shift in the angle of zero lift corresponds to an equal change in the tail angle of attack. Thus, the positive shift in the angle of zero lift, in effect, produces a positive increase in the angle of attack of the tail with a resulting nose-down pitching moment. The increment in elevator angle needed to offset this pitching moment was computed and is presented in figure 12(a). Comparing this computed increment with that needed for balance shows that the shift in angle of attack for zero lift will serve to explain most of the change in balance at low values of C_N above $M = 0.70$. Thus, it may be concluded that the nose-down pitching moment experienced above $M = 0.70$ was due to the change in the angle of zero lift of the wing.

Analysis of Pitching Moments During Dive

Problem (2), the increase in stability between $C_N = 0.2$ and $C_N = 0.4$, and problem (3), the abrupt pitch-up, will be considered in light of the dive shown in figure 6. In analyzing the results of this dive C_N and Mach number will be treated as the primary variables.

The equation for the pitching-moment coefficients about the airplane center of gravity, with a few [1]assumptions, may be expressed as

---

[1]It is assumed that velocity and acceleration along the lateral axis is zero, and that the thrust acts through the airplane center of gravity.

$$C_{m_{fus}} + \frac{a}{\bar{c}} C_N + \frac{z}{\bar{c}} C_X + C_{m_{c/4}} + C_{m_H} = \frac{B\left(\frac{d^2\theta}{d\tau^2}\right)}{qc\bar{S}} \qquad (1)$$

For an airplane in steady flight $\left(\frac{d^2\theta}{d\tau^2}\right) = 0$ or the airplane is in balance. The various terms of equation (1) will be considered individually with the intent of determining the cause of the increase in stability between $C_N = 0.2$ and 0.4 and also the cause of the pitch-up.

Fuselage pitching moment.- The pitching-moment coefficients of the fuselage calculated by the method of reference 3 are shown in figure 13(a). The fuselage critical Mach number at zero angle of attack from reference 4 was estimated to be 0.87. Since the Mach number for fuselage moment divergence would be still greater, it was assumed that the fuselage was operating below the critical. The correction for compressibility effects using reference 5 proved to be small (maximum $C_m = 0.010$) and therefore the uncorrected incompressible values of pitching-moment coefficients were used. When the values of fuselage pitching-moment coefficients were used, the fuselage was eliminated as a cause of the problems associated with the dive.

Pitching moments due to normal and longitudinal forces.- The effect of the normal-force coefficient C_N on the pitching coefficient is shown in figure 13(b). Its effect is relatively unimportant since the airplane center of gravity was close to the quarter-chord point of the mean aerodynamic chord.

The values of longitudinal-force coefficient C_X were obtained from the longitudinal accelerometer record and an estimate of the jet thrust. Its effect on C_m is shown in figure 13(c) and is also not important as regards the dive problems.

Wing pitching moment.- The wing-pressure measurements made during the dive allow an exact determination of the contribution of the wing toward the balance and stability of the airplane. Figure 13(d) presents the values of $C_{m_{c/4}}$ of the wing during the dive. Since all the values of $C_{m_{c/4}}$ are negative and since $dC_{m_{c/4}}/dC_N$ is negative at the higher lift coefficients, the wing could not have directly produced the pitch-up. However the change in $dC_{m_{c/4}}/dC_N$ from a positive value at C_N below 0.2 to a

negative value above $C_N = 0.2$ would serve to explain at least part of the stability increase between $C_N = 0.2$ and 0.4.

Tail pitching moment.- The pitching-moment coefficient of the airplane, tail off, may be found by summing the contributions of the various components. Thus

$$C_{m_{\text{tail off}}} = C_{m_{fus}} + \frac{a}{c} C_N + \frac{z}{c} C_X + C_{m_{c/4}} \qquad (2)$$

The pitching-moment coefficient of the tail is then, from equation (1):

$$C_{m_H} = \frac{B\left(\frac{d^2\theta}{d\tau^2}\right)}{qc\bar{S}} - C_{m_{\text{tail off}}} \qquad (3)$$

The tail-off pitching-moment coefficient is presented in figure 14. Also shown is the out-of-balance pitching-moment coefficient $B(d^2\theta/d\tau^2)/qS\bar{c}$ derived from the measured slope of the pitching-velocity curve of figure 6. From these two curves the pitching-moment coefficient produced by the tail was determined according to equation (3) and is presented in figure 15. The results indicate that the tail pitching moment became increasingly positive at the higher values of C_N up to the stall. Thus by a process of elimination it has been deduced that the tail pitching moment was the principal cause of the pitch-up.

Analysis of Horizontal-Tail Pitching Moment

It was shown that the action of the tail was the probable cause of the abrupt pitch-up. The purpose of the following analysis is to determine how this occurred.

The pitching-moment coefficient of the horizontal tail may be expressed as:

$$C_{m_H} = \frac{l}{\bar{c}} \frac{S_H}{S} \frac{q_H}{q} \left\{ \frac{\partial C_{L_H}}{\partial \alpha_H} \left[\alpha - \epsilon + i_t \times 57.3 \frac{l\left(\frac{d\theta}{d\tau}\right)}{V} \right] + \left(\frac{\partial C_{L_H}}{\partial \delta_e} \right) \delta_e \right\} \qquad (4)$$

By utilizing test results (unpublished data on file at the laboratory) of a 1/3-scale model of the horizontal tail in the Ames 16-foot high-speed wind tunnel the number of unknown variables is reduced to three; ϵ, α, and q_H/q. The possibility that any one

of these variables caused the abrupt pitch-up will now be considered. The method of analysis for α and q_H/q will be to solve for the variation that is required for each one of these variables to produce the tail pitching-moment-coefficient curve of figure 15, assuming reasonable values for the two remaining unknowns.

Downwash angle.- If it is assumed that the tail is close enough to the trailing edge of the wing and of small enough span so that the effect of the rolling up of the trailing vortices may be neglected, then the downwash angle may be expressed as

$$\epsilon = 57.3 \frac{w}{V} \cong 57.3 \int \frac{q}{q_H} k \, c_n c \, dy \qquad (5)$$

where the integral is evaluated over the center section. If $q_H/q = 1.0$, the downwash angle will vary linearly with the wing center-section loading $\int \frac{c_n c}{\bar{c}} d\left(\frac{2y}{b}\right)$. Other wind-tunnel tests indicate that, at a constant lift coefficient, Mach number has a minor effect on downwash.

The integrated center-section loading obtained from the spanwise loadings of reference 1 is presented in figure 16. Also shown are values obtained during the dive which are slightly larger than those indicated from the low-speed results, probably due to the fact that the ailerons were deflected upward. At any rate, there is insufficient increase in downwash to produce the pitch-up.

From wind-tunnel tests[2] of a 1/3-scale model of the test airplane the derived downwash angle variation with C_N for a range of Mach numbers from 0.3 to 0.85 was obtained and is presented in figure 17. No Mach number effect is apparent. The variation of ϵ with C_N thus obtained was corrected for the increase in center-section loading and the corrected variation as used in the subsequent analysis is also shown in figure 17.

Angle of attack.- To determine the variation of α with C_N required to produce the tail pitching-moment results shown in figure 15, it was assumed that (1) $q_H/q = 1.0$, (2) the variation of ϵ with C_N was as shown in figure 17, and (3) the horizontal-tail characteristics were as determined in the wind-tunnel tests of the isolated tail. For convenience in making the analysis, these wind-tunnel data were plotted as the variation of C_{L_H} with Mach number

[2]Unpublished data on file at the laboratory.

for the values of δ_e corresponding to specific points during the dive. A typical example is shown in figure 18.

Using the tail characteristics as measured in the wind tunnel, the values of α_H needed to produce the values of C_{m_H} of figure 15 were determined. Then

$$\alpha = \alpha_H + \epsilon - i_t - 57.3 \frac{l\left(\frac{d\theta}{dt}\right)}{V} \qquad (6)$$

which (in light of the assumptions made) allows the values of α to be determined. The variation of α with C_N thus derived is shown in figure 19. This variation is required to produce the longitudinal characteristics of the dive. Comparison of this lift curve with that derived from extrapolation of the wind-tunnel tests of reference 2 (fig. 20) indicates dissimilarities. For the portion of the dive before the pitch-up, the difference in slopes tends to eliminate the lift curve as the cause of the increased stability. In regard to the pitch-up, the results shown in figure 20 indicate that the effect of decreasing the Mach number as C_N is increasing from 0.5 to 0.89 is to markedly increase the slope of the curve. This would agree with the steep slope in figure 19 between $C_N = 0.5$ and 0.7. For C_N greater than 0.7, however, the reduction in α with increasing C_N is improbable. Therefore, it may be concluded that the variation of α with C_N may explain part of the reduction in stability during the pitch-up due to the fact that the airplane Mach number was decreasing, but it does not entirely explain the latter portion of the pitch-up above 0.7 C_N.

Dynamic pressure at the tail.- A reduction in dynamic pressure over the tail occurs due to the wing wake. This effect can become important above the critical Mach number of the wing when a pronounced flow separation is present. This reduction in dynamic pressure has two effects: (1) It reduces the ΔC_m obtainable with a given ΔC_{L_H} as can be seen in equation (4), and (2) it causes the Mach number at the tail to be lower than the airplane Mach number. The reduction in q_H/q and Mach number at the tail can be seen in figure 21 as a function of loss in total-head pressure. Thus at $M = 0.85$, a loss in total-head pressure sufficient to produce a $q_H/q = 0.90$ lowers the Mach number at the tail approximately 0.04. It may be seen in figure 18 that such a reduction in Mach number could produce a much larger change in tail load than that due to the effect of the change in q_H/q itself. This is due to the large effect of Mach number on $\partial C_{L_H}/\partial \delta_e$ and $\partial C_{L_H}/\partial \alpha_H$ above $M = 0.80$.

For the purposes of analysis certain assumptions have been made:

1. Variation of ϵ with C_N is as shown in figure 17.

2. Variation of α with C_N is as shown in figure 20. This variation was derived from an extrapolation of the wind-tunnel results of reference 2.

3. Tail characteristics are as determined from wind-tunnel tests of the isolated tail.

These assumptions coupled with measured values allow α_H to be determined, leaving only q_H/q, $\partial C_{L_H}/\partial \alpha_H$, and $\partial C_{L_H}/\partial \delta_e$ as unknowns in equation (4). Since all these were shown to be a function of the total-head loss over the tail, the required variation of q_H/q was found by a series of successive approximations. The variation of q_H/q and Mach number at the tail required to explain the abrupt pitch-up is presented in figure 22. From this it may be seen that the required reduction in dynamic pressure increases with increase in C_N. This is quite plausible, since at higher angles of attack the wake becomes broader and the tail moves toward the wake.

To demonstrate this more clearly the wing wake at the tail for the test airplane at $M = 0.85$ was estimated for a low value of C_N and also for the value of C_N at the beginning of the pitch-up. These estimates are shown in figure 23 and are based on wind-tunnel surveys of a thinner wing and should be considered only roughly quantitative. They do show the liklihood of wake changes at the tail.

In addition to the reduction of the dynamic pressure, the wake produces a velocity gradient in the vertical direction at the tail. This velocity gradient will produce a lift on the tail dependent upon the thickness of the tail and the velocity gradient. This subject has been treated in references 6 and 7.

Summary of Balance Changes and Apparent Stability

A shift in the angle of attack for zero lift, changes in elevator effectiveness, and changes in stabilizer effectiveness produce changes in the elevator angle required for balance at various Mach numbers. If C_N and Mach number are both varying, the changes in balance can result in an apparent change in stability $\Delta C_m/\Delta C_N$. When both C_N

and Mach number are increasing, an increase in the angle of attack for zero lift produces an apparent increase in stability. This accounts for part of the increase in stability during the dive recovery between $C_N = 0.2$ and 0.4. When C_N is increasing and the Mach number is decreasing, the reduction in zero lift angle causes an apparent decrease in stability, which partially explains the abrupt pitch-up.

The effect on the airplane balance due to changes of elevator effectiveness and stabilizer effectiveness is dependent on the angle of attack of the tail, the elevator deflection, and the relative changes in effectiveness with Mach number. For the dive in question, the net effect of the decreasing airplane Mach number was to produce a nose-up pitching moment; and because C_N was increasing, an apparent decrease in stability resulted. It was previously shown that, due to the wing wake, the Mach number at the tail probably decreased more rapidly than the airplane Mach number, greatly increasing this effect.

The combination of these changes in the apparent stability and the reduction in Mach number over the tail serves to explain the pitch-up below $C_N = 0.75$. Above this value this explanation fails to account for all of the necessary tail pitching moment and at $C_N = 0.89$ it explains only about 60 percent of the required moment, leaving an unexplained pitching-moment coefficient of 0.030.

A reasonable explanation for the inability to satisfactorily explain the entire pitch-up lies in the probable inaccuracies in the results during the final and most rapid stage of the maneuver. For example, assuming an error in Mach number of 0.015 (the estimated accuracy) when $C_N = 0.89$, the resulting shift in angle for zero lift would have produced an increment of pitching-moment coefficient of 0.040.

The longitudinal problems thus appear to rise from the effect of Mach number on the angle of attack for zero lift and elevator and stabilizer effectiveness. The use of a symmetrical wing would reduce the shift with Mach number in the angle of attack required for a given lift coefficient at least for moderate lift coefficients. This would reduce the increment in elevator angle needed for balance and thereby proportionately reduce the effect of a change in elevator effectiveness on balance. A partial solution would be to alleviate the effects of Mach number on elevator effectiveness and stabilizer effectiveness. The use of a swept-back tail surface would accomplish this purpose as may be observed in figure 24 which compares the

elevator effectiveness and stabilizer effectiveness at high Mach numbers for the standard tail and for the tail swept back.

CONCLUDING REMARKS

This report explains the abrupt pitching-up of the airplane which occurred during a 0.866 Mach number dive. Some additional related stability problems have also been included.

One of these additional problems, the nose-down tendency of the airplane above $M = 0.70$, was shown to be due to the positive shift in the angle of attack for zero lift of the wing. At any given value of C_N, this shift served to increase the angle of attack of the tail and produced a diving moment.

Another problem, the increase in stability which occurred between $C_N = 0.2$ and 0.4, was attributed partly to an increase in stability of the airplane, tail off, and partly to the balance changes associated with an increasing airplane Mach number.

It was shown that the action of the tail was responsible for the pitch-up. The negative shift in angle for zero lift and increase in elevator effectiveness as the airplane Mach number decreased produced a nose-up change in balance. The presence of the wing wake produced an additional decrease in Mach number at the tail which further increased the elevator effectiveness and the nose-up pitching moment.

It was suggested that utilization of a symmetrical wing and a swept tail would alleviate the longitudinal-stability problems encountered.

Ames Aeronautical Laboratory,
National Advisory Committee for Aeronautics,
Moffett Field, Calif.

REFERENCES

1. Brown, Harvey H. and Clousing, Lawrence A.: Wing Pressure-Distribution Measurements Up to 0.866 Mach Number in Flight on a Jet-Propelled Airplane. NACA TN No. 1181, 1947.

2. Cleary, Joseph W. and Gray, Lyle J.: High-Speed Wind-Tunnel Tests of a Model Pursuit Airplane and Correlation with Flight Test Results. NACA RM No. A7I16, 1947.

3. Multhopp, H.: Aerodynamics of the Fuselage. NACA TM No. 1036, 1942.

4. Robinson, Russell G. and Wright, Ray H.: Estimation of Critical Speeds of Airfoils and Streamline Bodies. NACA ACR, Mar. 1940.

5. Lees, Lester: A Discussion of the Application of the Prandtl-Glauert Method to Subsonic Compressible Flow Over a Slender Body of Revolution. NACA TN No. 1127, 1946.

6. Ruden, P.: NACA Airfoils in the Vicinity of Rectangular Jets and Wake Profiles. 1939 Jahrbuch.

7. Ruden, P.: New Investigations on the Influence of Non-Uniform Distributions of Total Head Upon Parts of the Airplane, LGL, Bericht 117.

TABLE I.- BASIC DIMENSIONAL DATA OF THE TEST AIRPLANE

Item	Wing	Horizontal tail
Area, sq ft	237	43.5
Span, ft	38.9	15.6
Aspect ratio	6.39	5.59
Taper ratio	0.364	0.308
Mean aerodynamic chord, ft	6.72	3.08
Dihedral of trailing edge, deg	3.83	0
Incidence, root chord, deg	1	1.50
Incidence, tip chord, deg	-0.50	1.50
Root section	NACA 65_1-213 (a=0.5)	NACA 65-010
Tip section	NACA 65_1-213 (a=0.5)	NACA 65-010
Percent chord having common plane	52	75
Tail length (from 0.25 M.A.C. wing to 0.25 M.A.C. tail), ft	—	14.90

TABLE II.- ORDINATES OF NACA 65_1-213 (a = 0.5) AIRFOIL
[All stations and ordinates in percent chord]

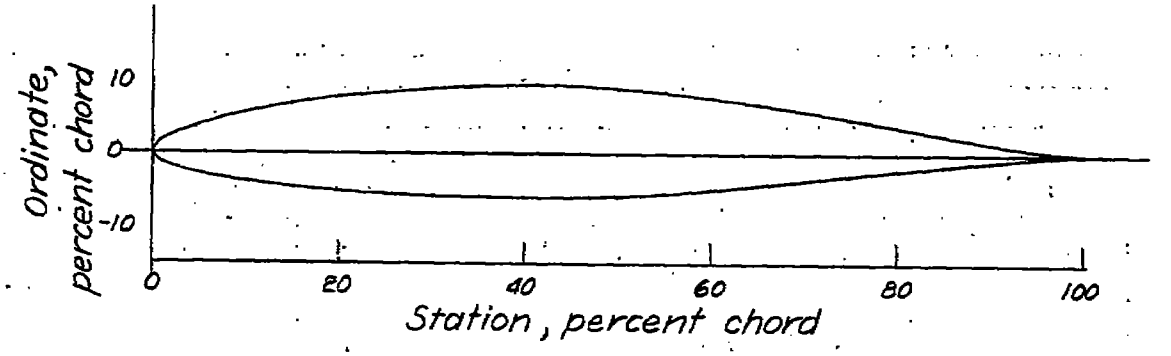

Upper surface		Lower surface	
Station	Ordinate	Station	Ordinate
0	0	0	0
.38	1.06	.62	-.92
.62	1.29	.88	-1.10
1.10	1.64	1.40	-1.35
2.34	2.28	2.66	-1.76
4.81	3.26	5.19	-2.38
7.31	4.02	7.69	-2.84
9.80	4.67	10.20	-3.22
14.81	5.71	15.19	-3.82
19.83	6.51	20.17	-4.26
24.86	7.12	25.14	-4.59
29.89	7.56	30.11	-4.82
34.92	7.85	35.08	-4.96
39.96	7.98	40.04	-5.01
45.01	7.94	44.99	-4.95
50.07	7.71	49.93	-4.77
55.11	7.26	54.89	-4.47
60.13	6.63	59.87	-4.07
65.14	5.89	64.86	-3.60
70.13	5.04	69.87	-3.06
75.11	4.14	74.89	-2.49
80.09	3.19	79.91	-1.88
85.06	2.24	84.94	-1.29
90.04	1.33	89.97	-.72
95.01	.53	94.99	-.24
100.00	0	100.00	0

L. E. radius: 1.174. Slope of radius through L. E.: 0.084

NATIONAL ADVISORY
COMMITTEE FOR AERONAUTICS

TABLE III.- ORIFICE LOCATIONS ON WINGS OF THE TEST AIRPLANE
[Given in percent of chord]

Left wing									
Upper surface					Lower surface				
Orifice no.	Spanwise station, in. from center line of airplane				Orifice no.	Spanwise station, in. from center line of airplane			
	65	105.25	152	207		65	105.25	152	207
1	0.68	0.72	0.32	0.36	1	0.69	0.69	0.39	0.25
2	1.47	1.55	.95	1.43	2	1.48	1.47	1.05	1.12
3	2.79	2.69	2.20	2.61	3	2.87	2.81	2.17	2.23
4	5.31	5.25	4.62	5.09	4	5.26	5.34	4.60	4.86
5	10.32	10.25	9.65	10.02	5	10.20	10.34	9.57	11.43
6	16.24	16.62	15.49	16.02	6	16.30	16.23	15.49	16.69
7	22.58	23.32	22.73	23.10	7	23.07	23.68	22.59	23.43
8	26.12	25.84	25.93	26.13	8	26.19	25.95	25.88	26.31
9	33.23	33.97	34.33	34.19	9	33.54	33.87	34.19	34.28
10	41.16	42.09	40.62	41.73	10	41.40	41.84	41.33	41.78
11	45.78	46.53	48.70	48.78	11	45.93	46.50	48.24	47.89
12	54.13	55.96	53.76	55.23	12	56.13	54.97	53.76	55.10
13	59.18	59.89	58.78	60.12	13	59.59	59.99	58.88	60.03
14	64.14	64.60	63.96	64.96	14	64.23	65.02	63.56	65.16
15	69.12	69.56	68.68	75.61	15	69.51	72.59	67.63	———
16	73.38	76.88	78.41	80.18	16	71.87	76.47	78.59	79.94
17	79.11	79.83	83.30	85.14	17	79.09	79.96	83.51	85.02
18	83.03	84.58	89.93	90.27	18	82.90	85.12	90.14	93.04
19	89.14	88.93	93.24	95.25	19	89.15	88.76	93.16	———
20	94.19	94.39	———	———	20	94.09	95.06	———	———
Section chord, feet	7.46	6.40	5.18	3.73	Section chord, feet	7.46	6.40	5.18	3.73

NATIONAL ADVISORY
COMMITTEE FOR AERONAUTICS

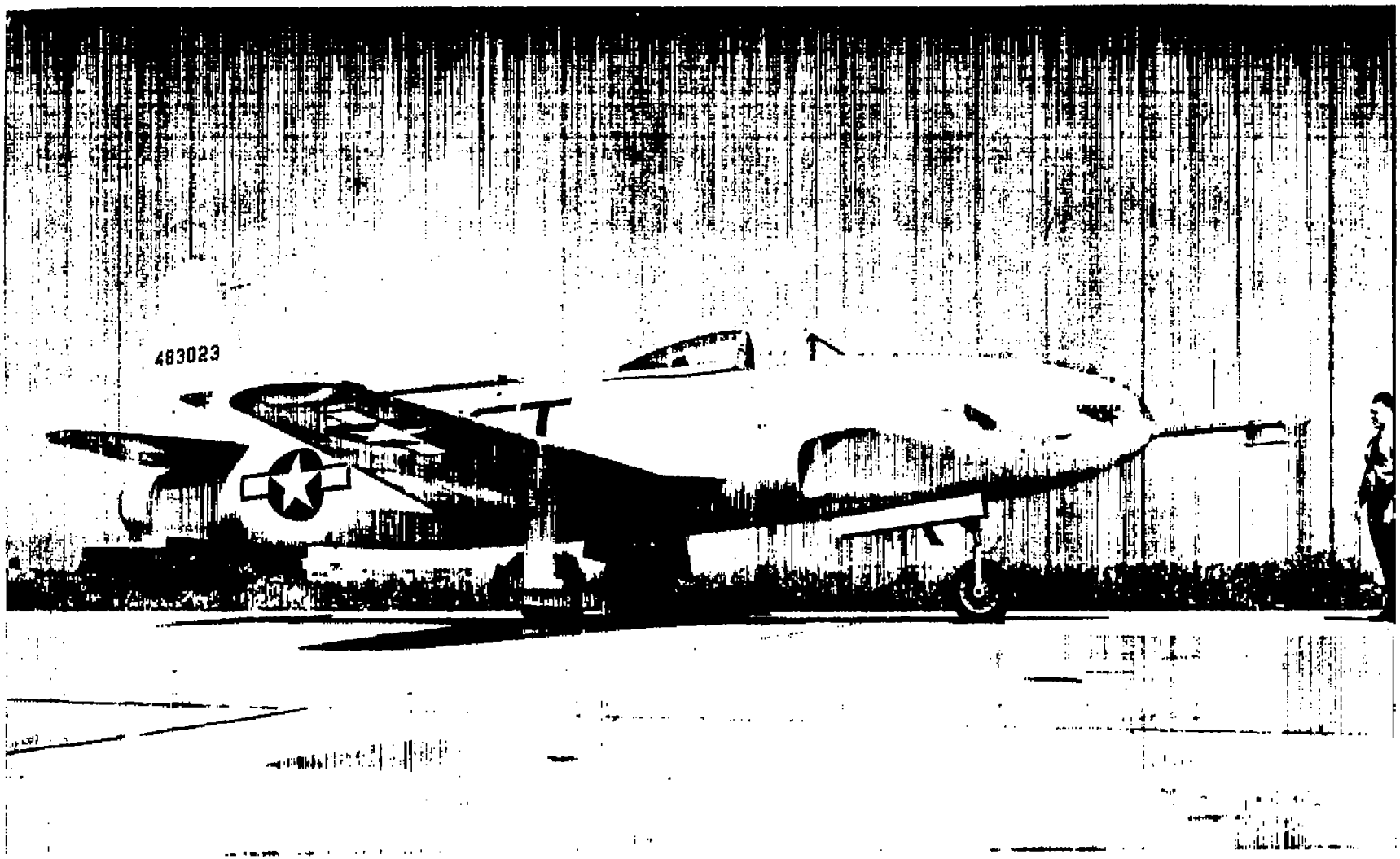

Figure 1.- Three-quarter side view of the test airplane.

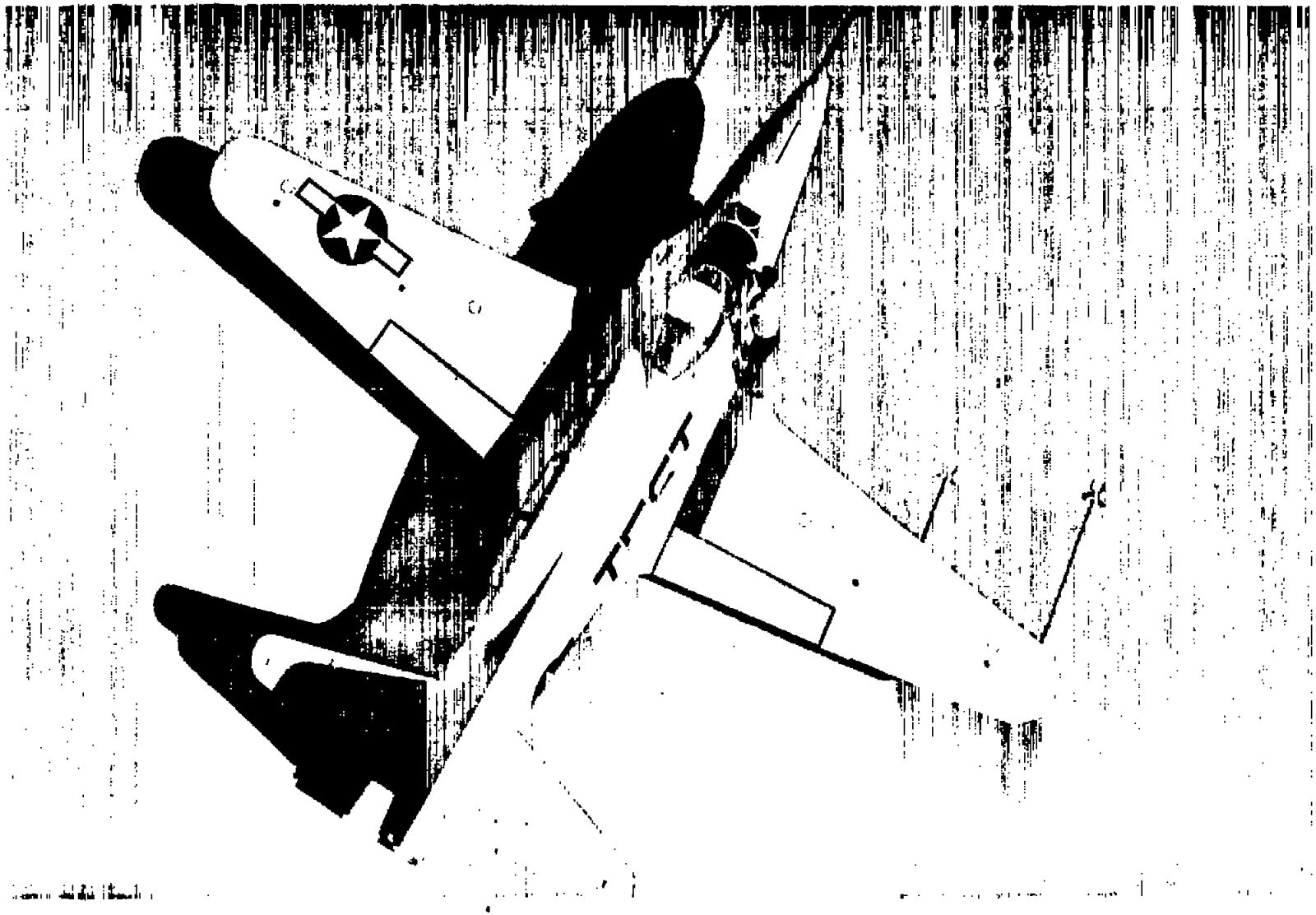

Figure 2.- Plan view of the test airplane.

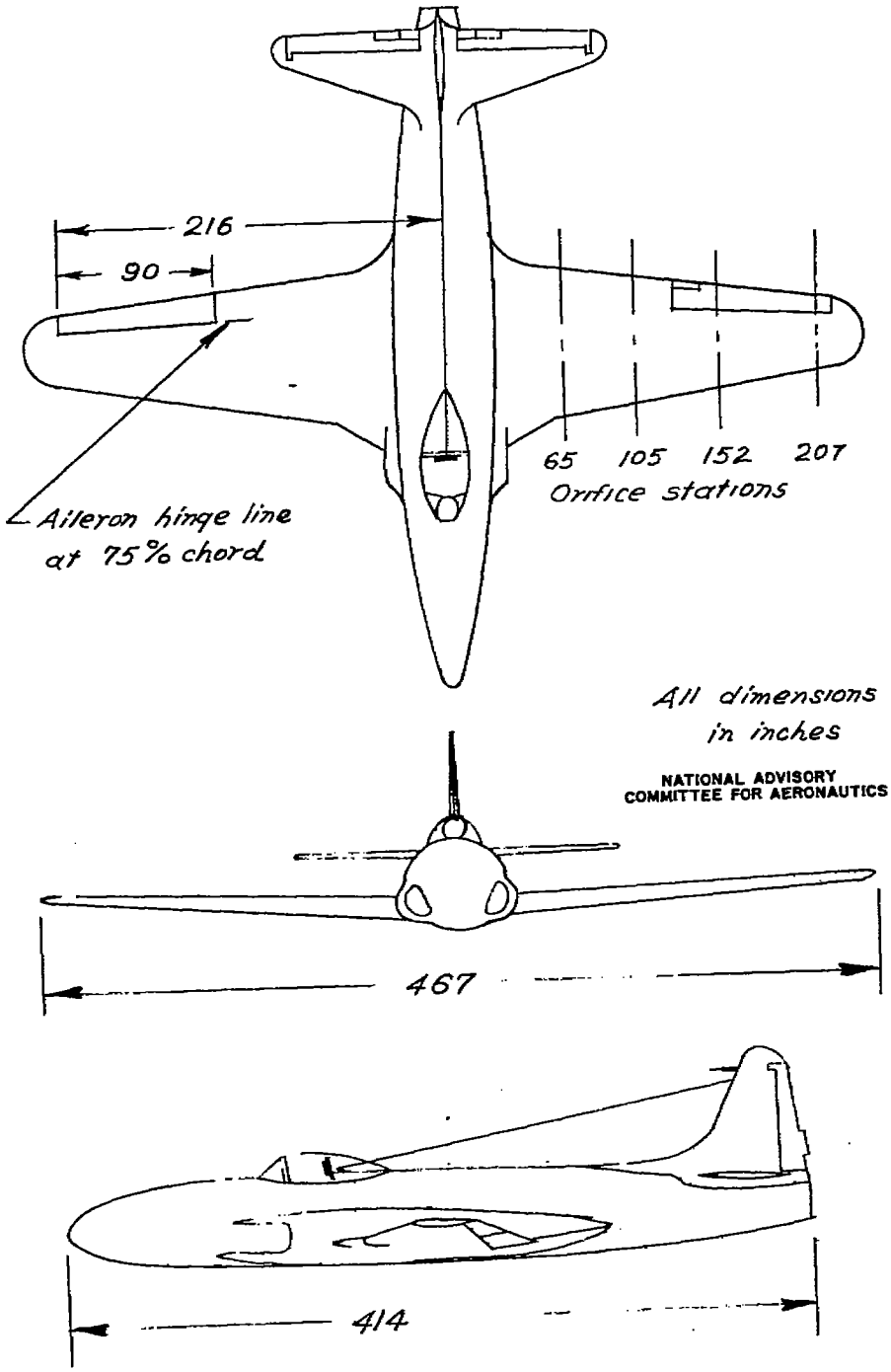

Figure 3. — Three-view drawing of the test airplane.

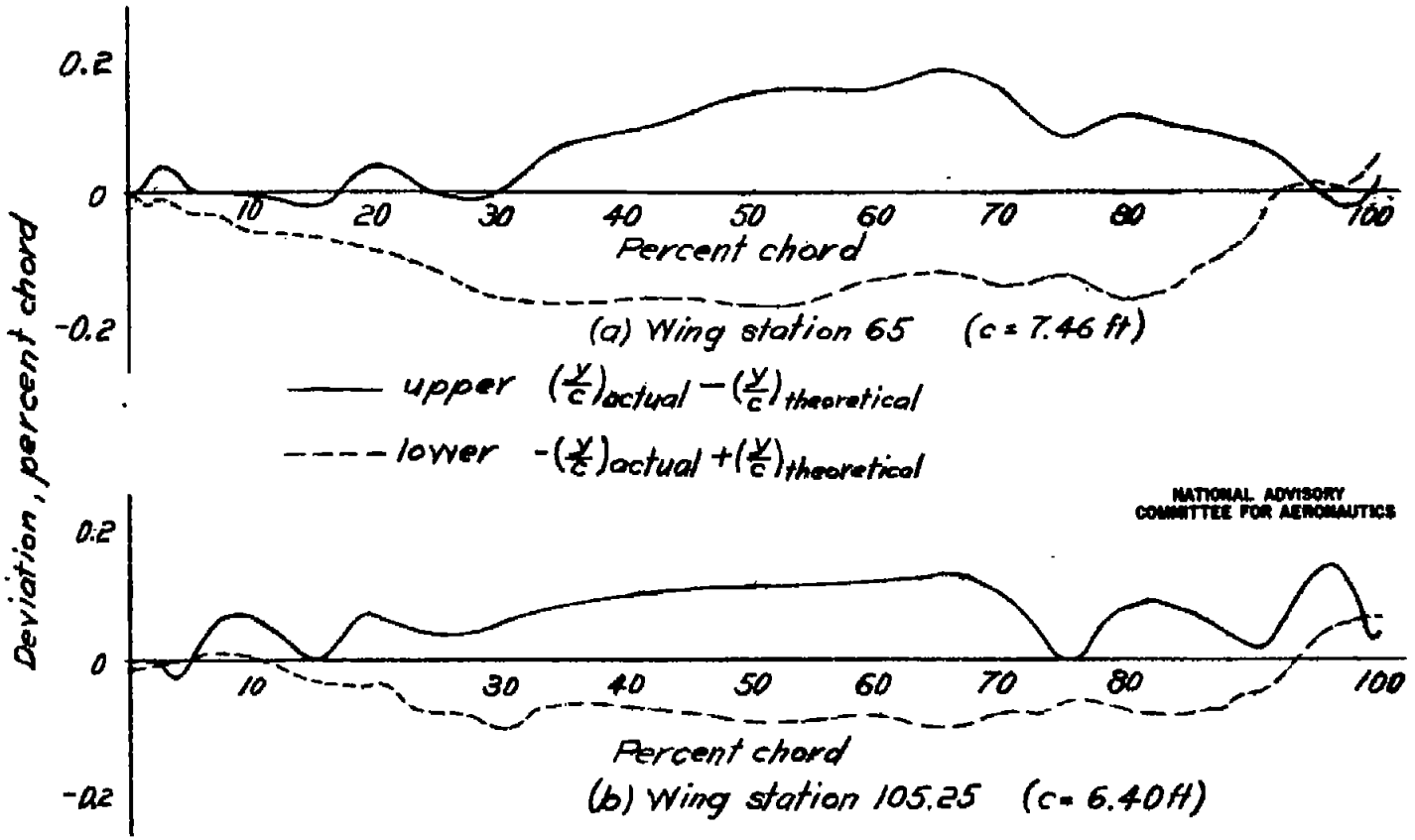

Figure 4.— Deviation of actual wing contour from theoretical airfoil at various spanwise locations.

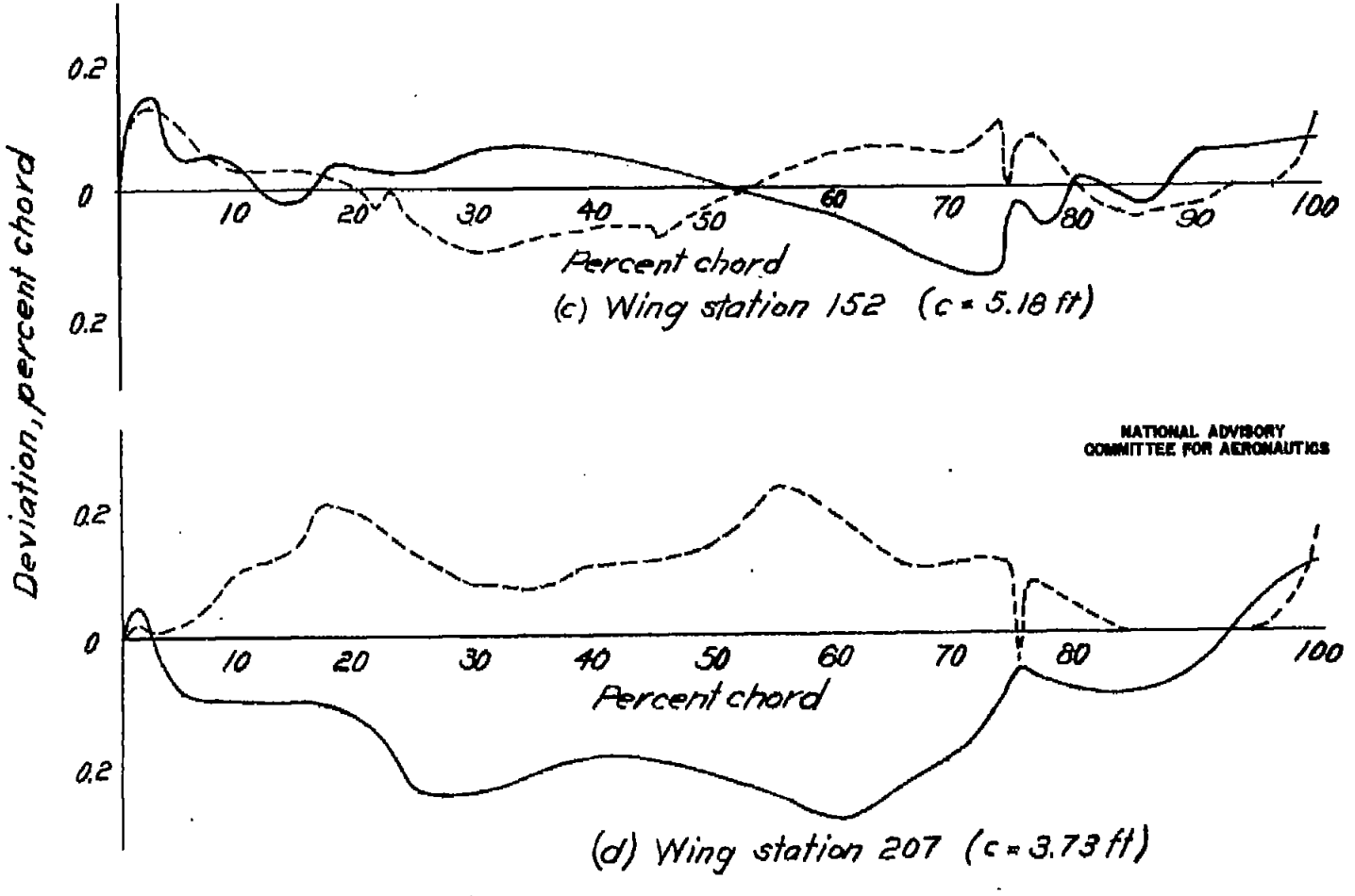

Figure 4.– Concluded.

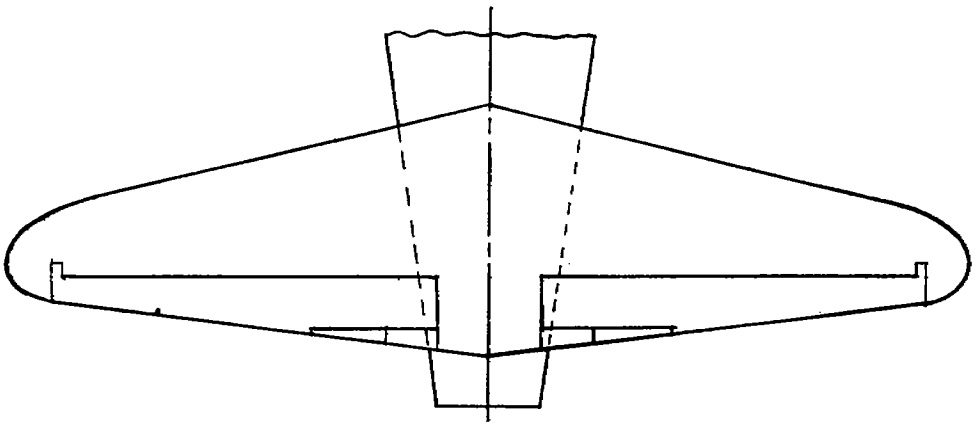

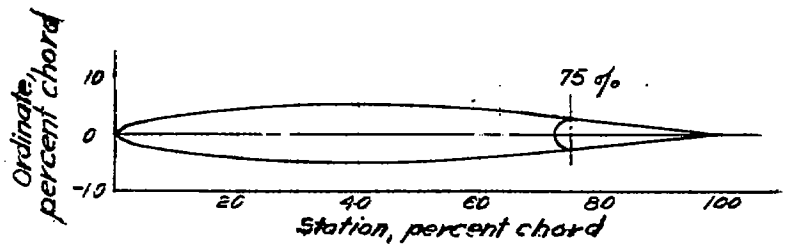

Station	Ordinate	Station	Ordinate
1.25	1.15	40.0	5.00
2.5	1.56	50.0	4.80
5.0	2.17	60.0	4.115
7.5	2.64	70.0	3.115
10.0	3.04	80.0	2.08
20.0	4.145	90.0	1.04
30.0	4.76	100	0
L. E. radius: 0.687			
T. E. angle: 11.84°			

NATIONAL ADVISORY
COMMITTEE FOR AERONAUTICS

Figure 5.- Plan form of horizontal tail of subject airplane and ordinates for the modified NACA 65_1-010 airfoil with straight side elevator.

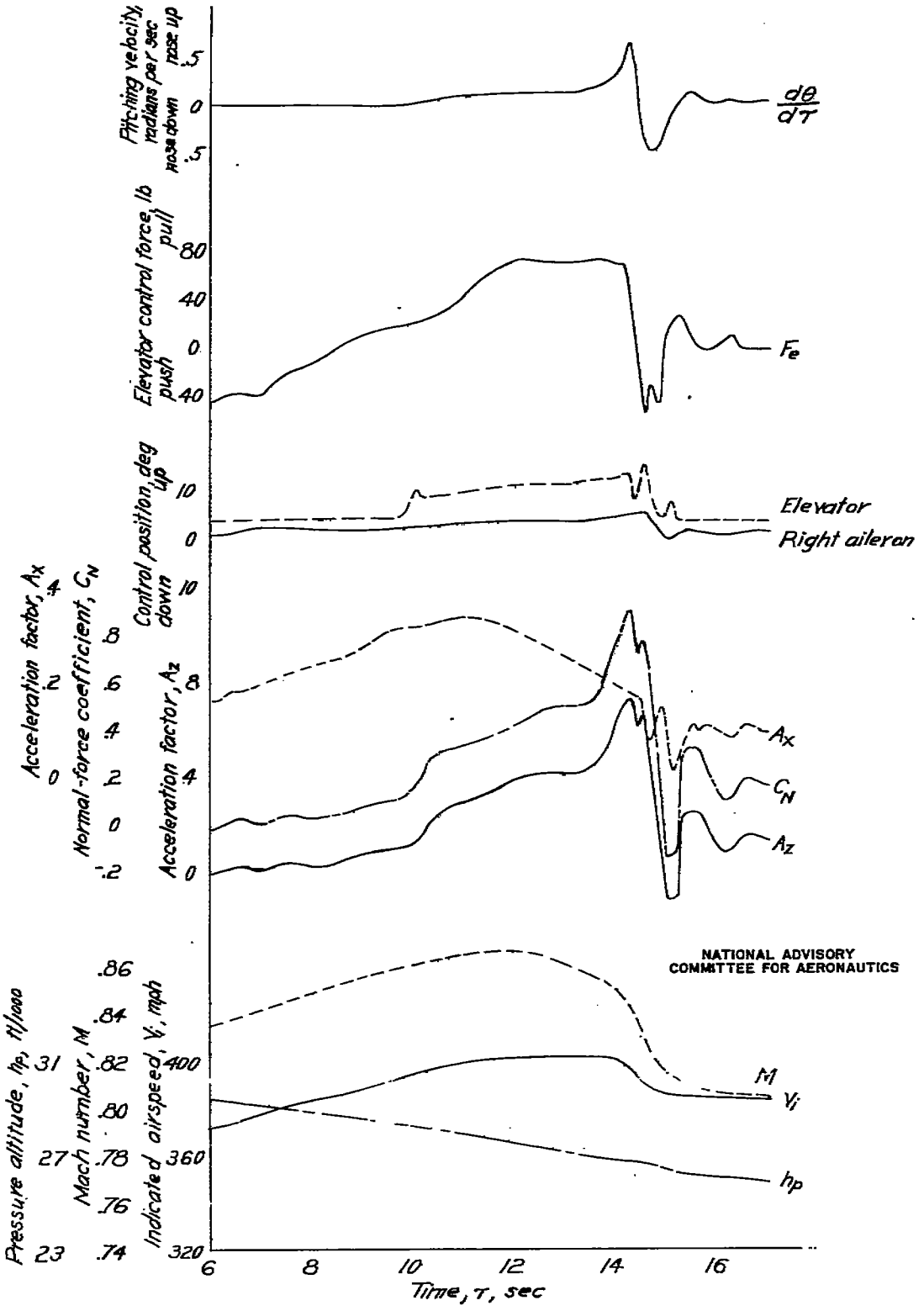

Figure 6.— Time history of dive recovery

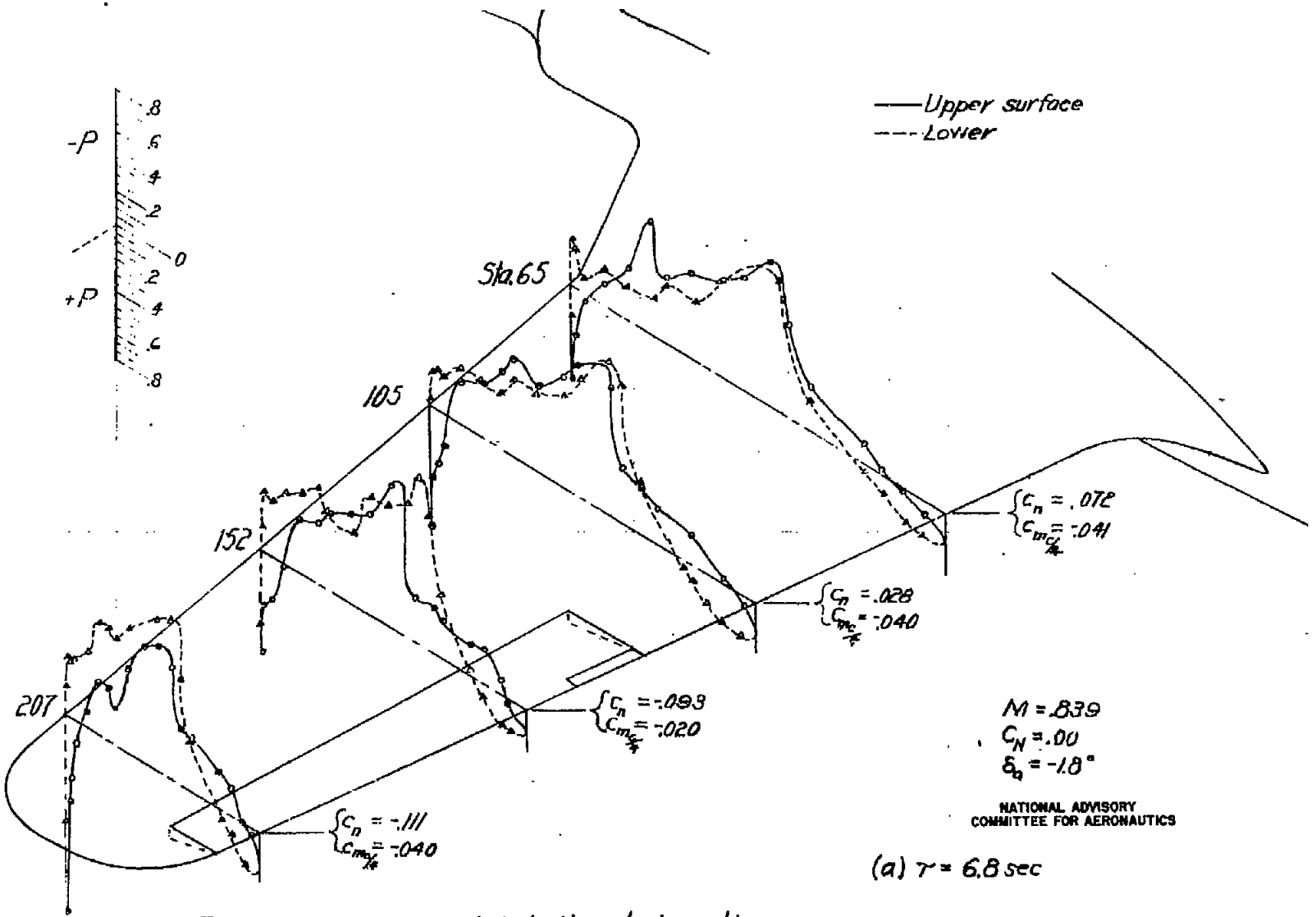

Figure 7.– Wing pressure distribution during dive recovery.

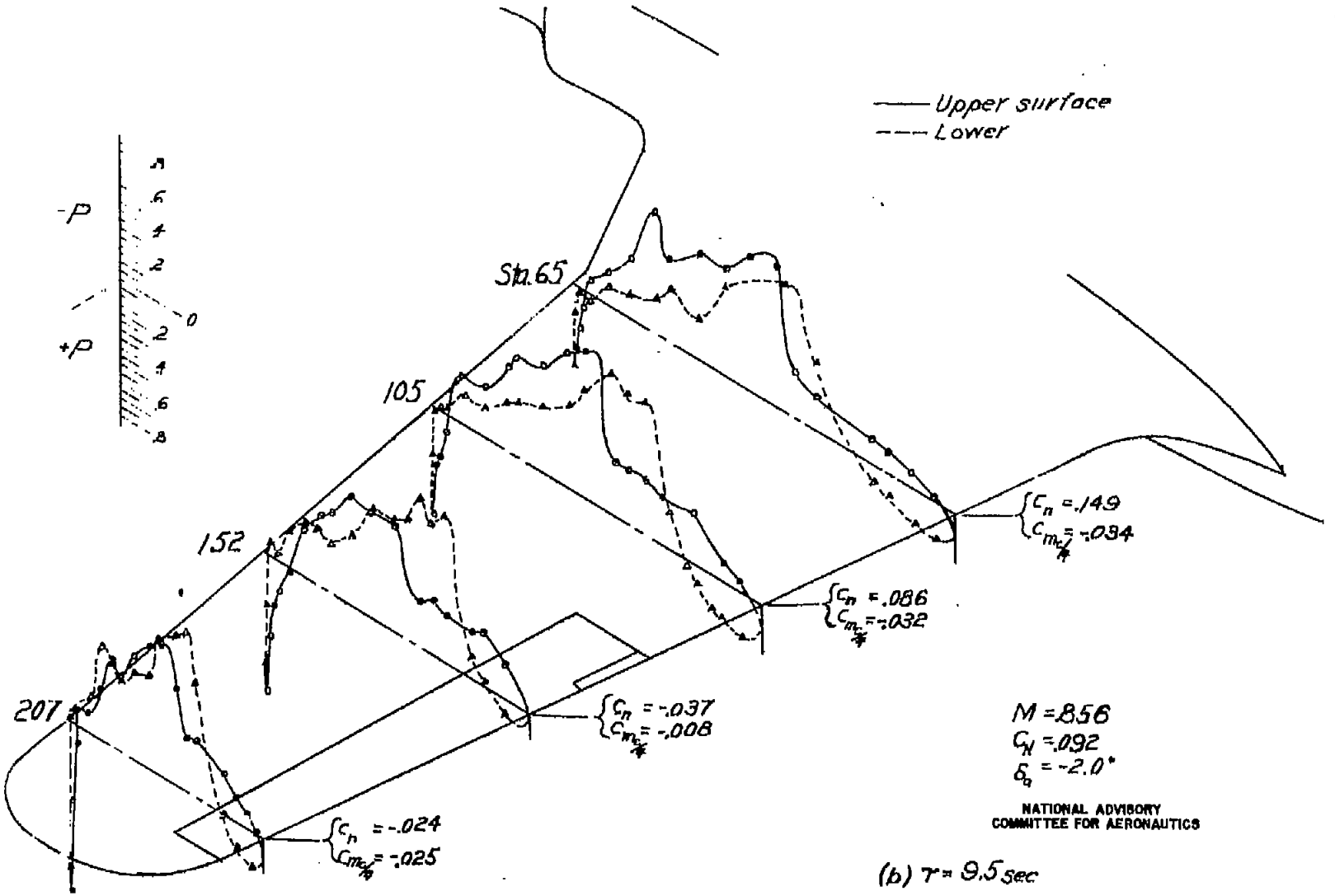

Figure 7. — Continued.

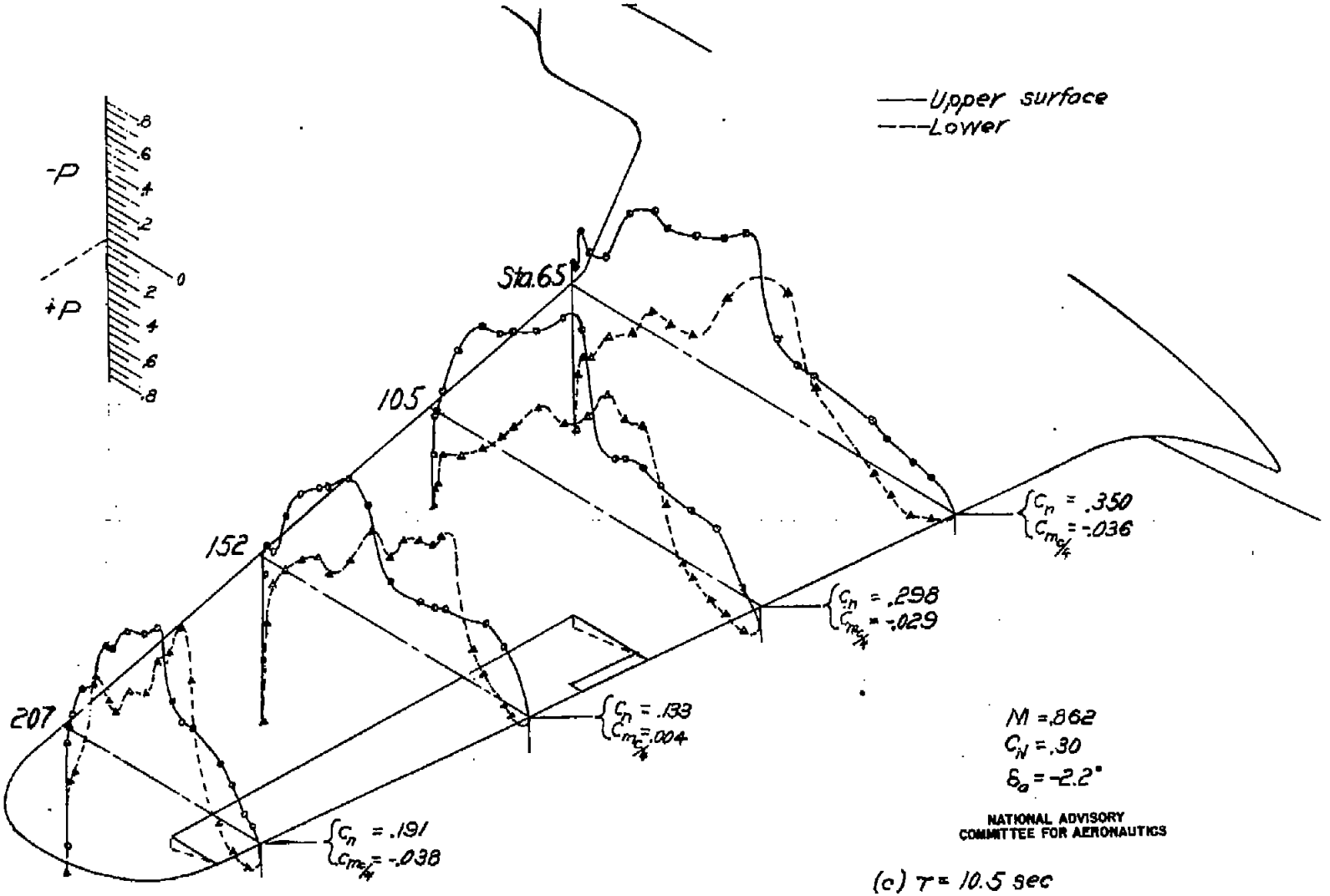

Figure 7.—Continued.

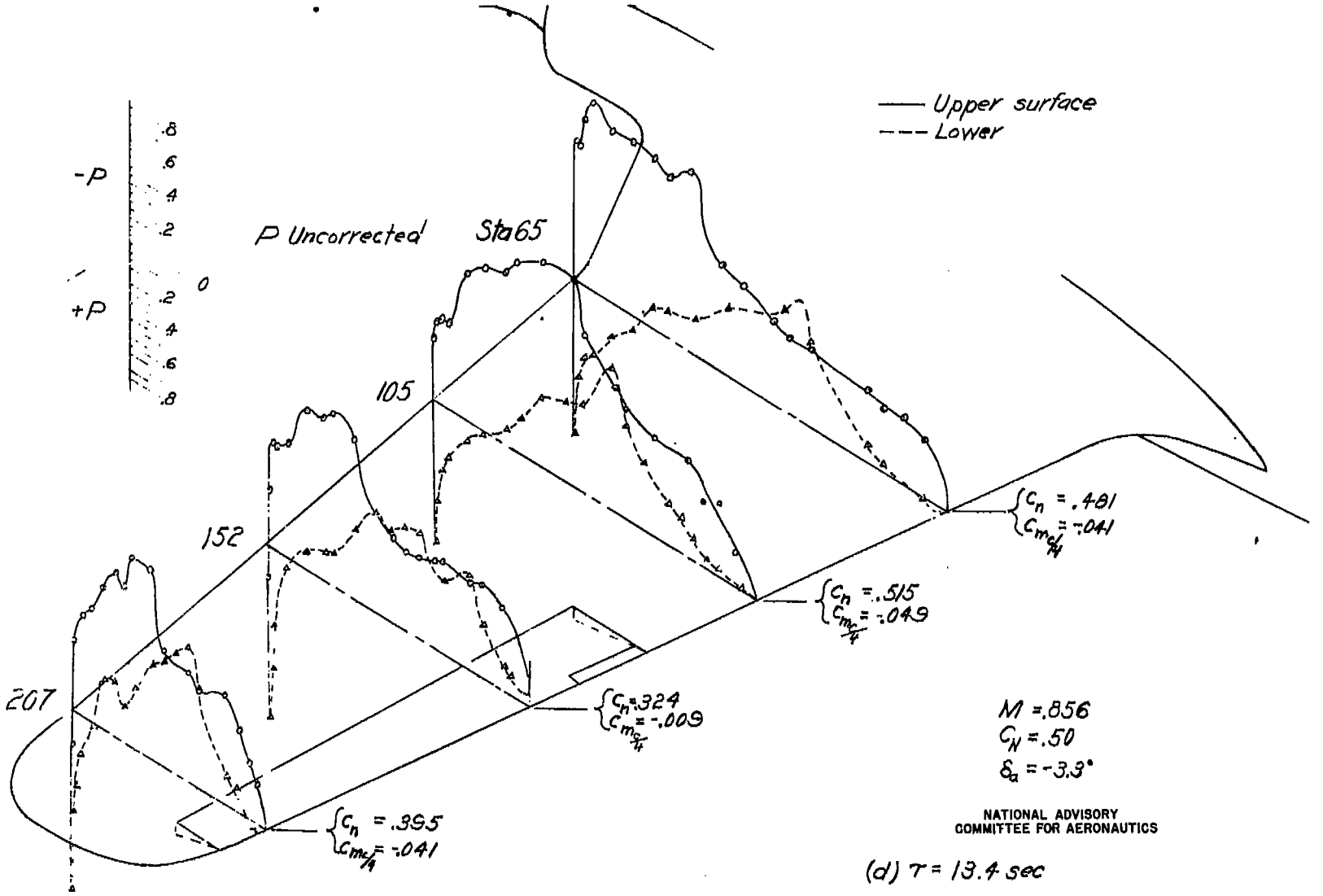

Figure 7. — Continued.

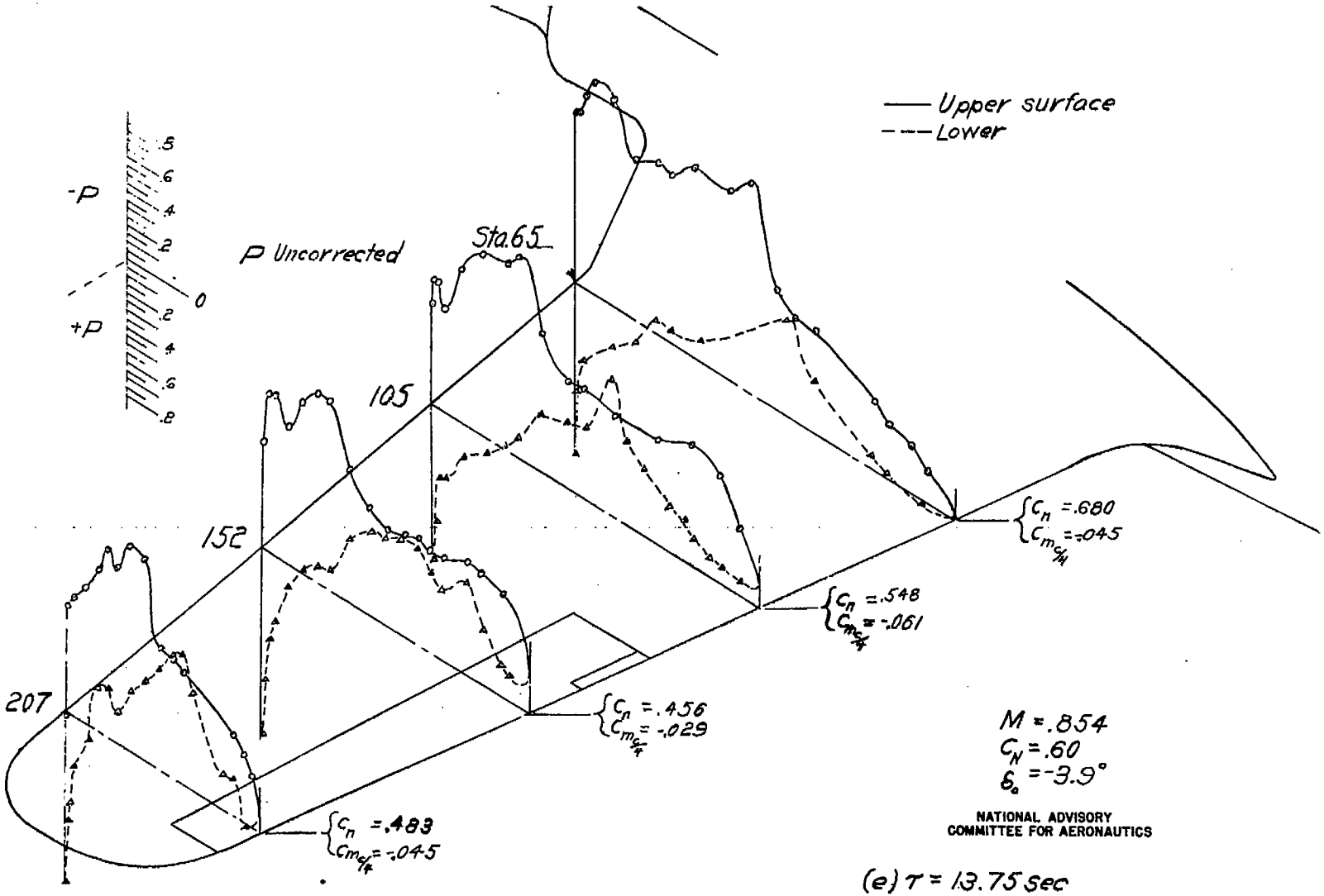

Figure 7. – Continued.

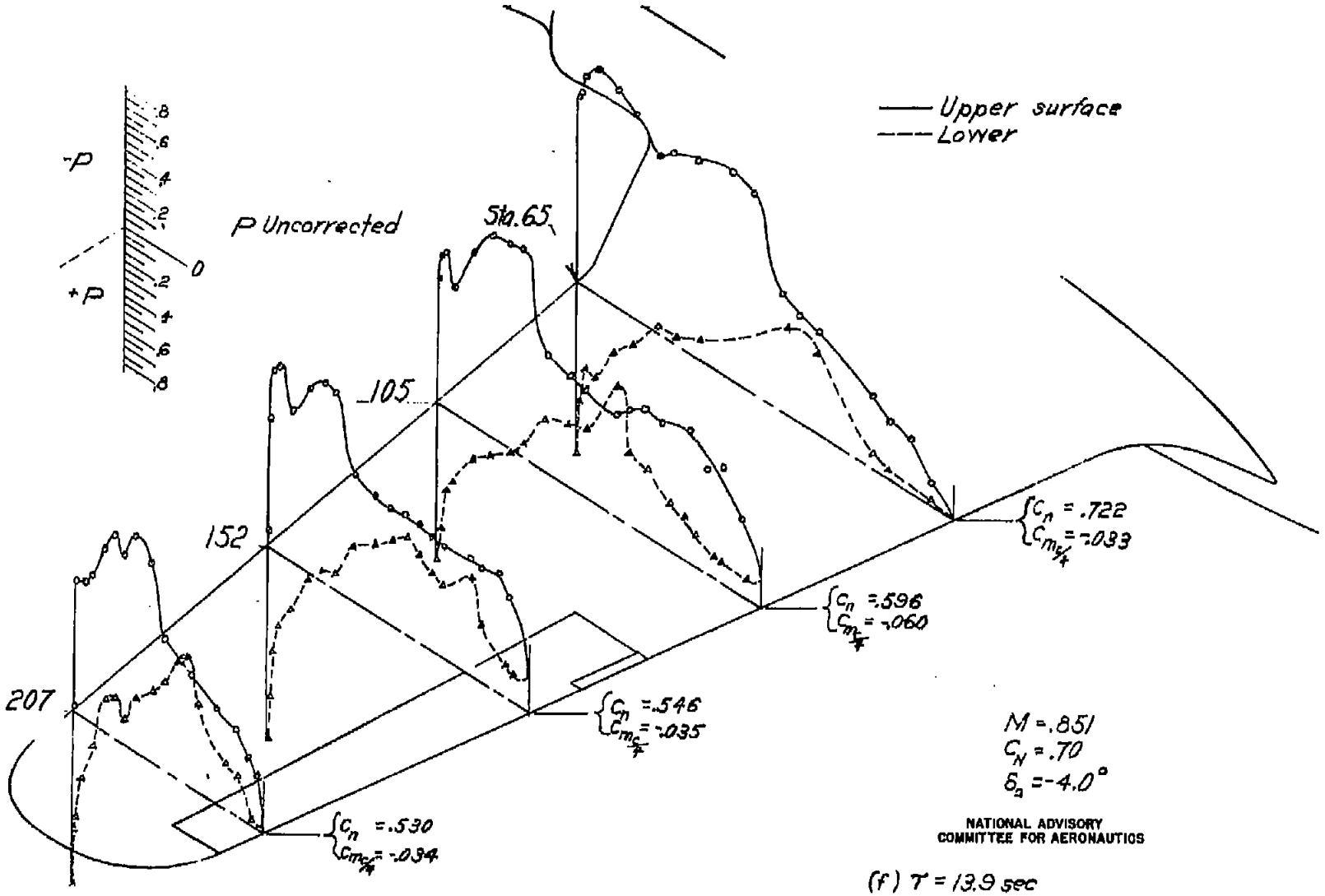

Figure 7.— Continued.

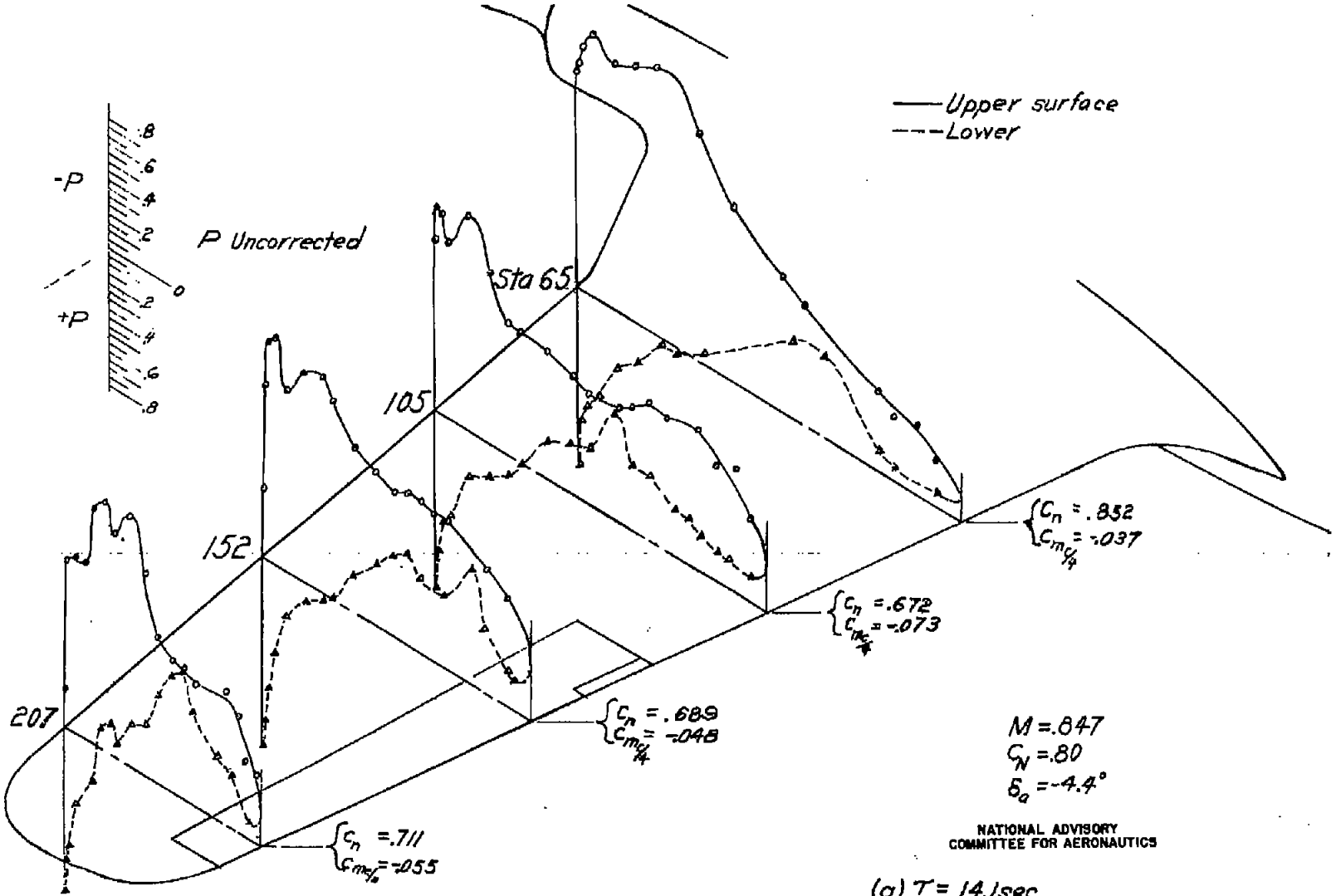

Figure 7.—Continued.

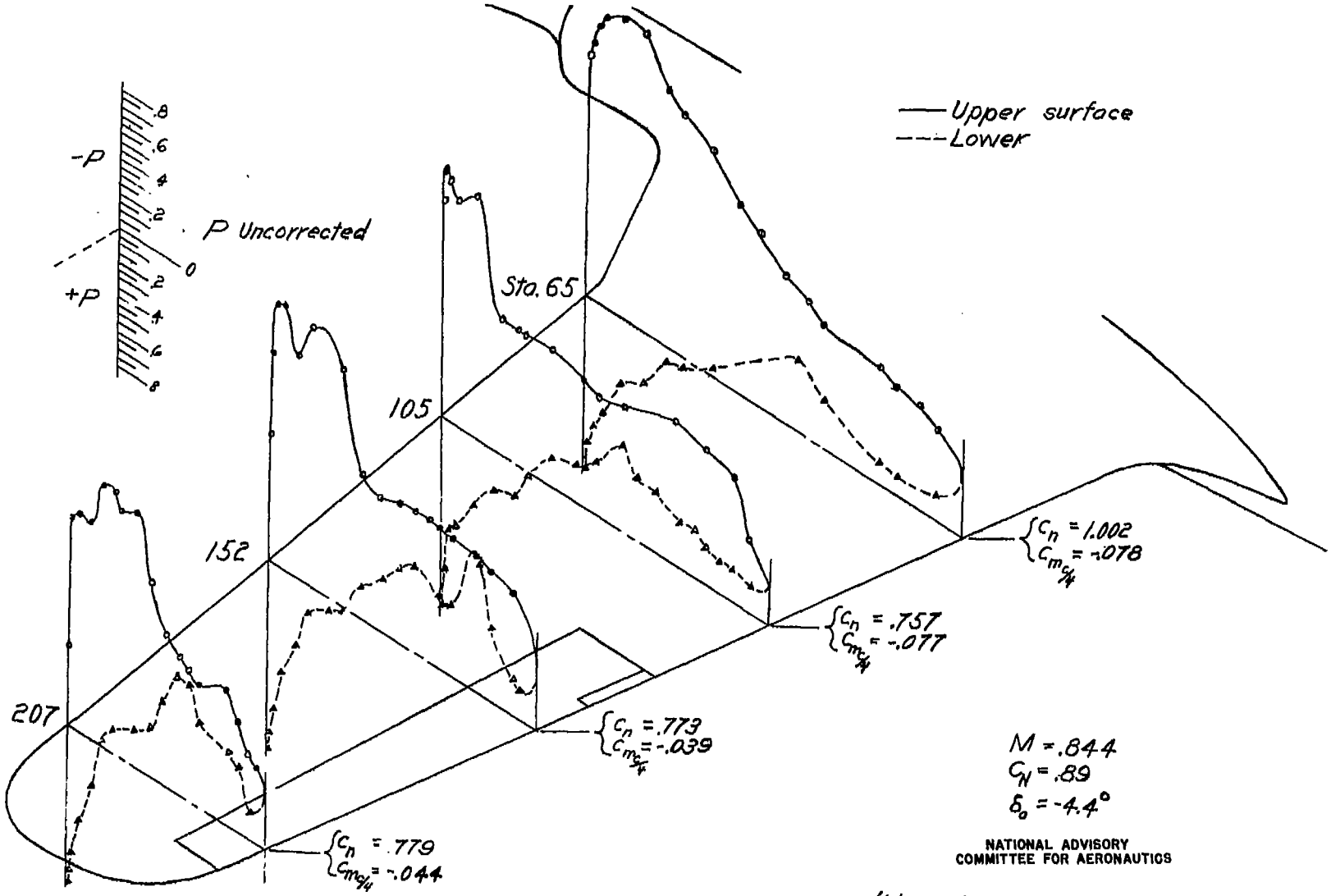

(h) $T = 14.25$ sec

Figure 7. – Continued.

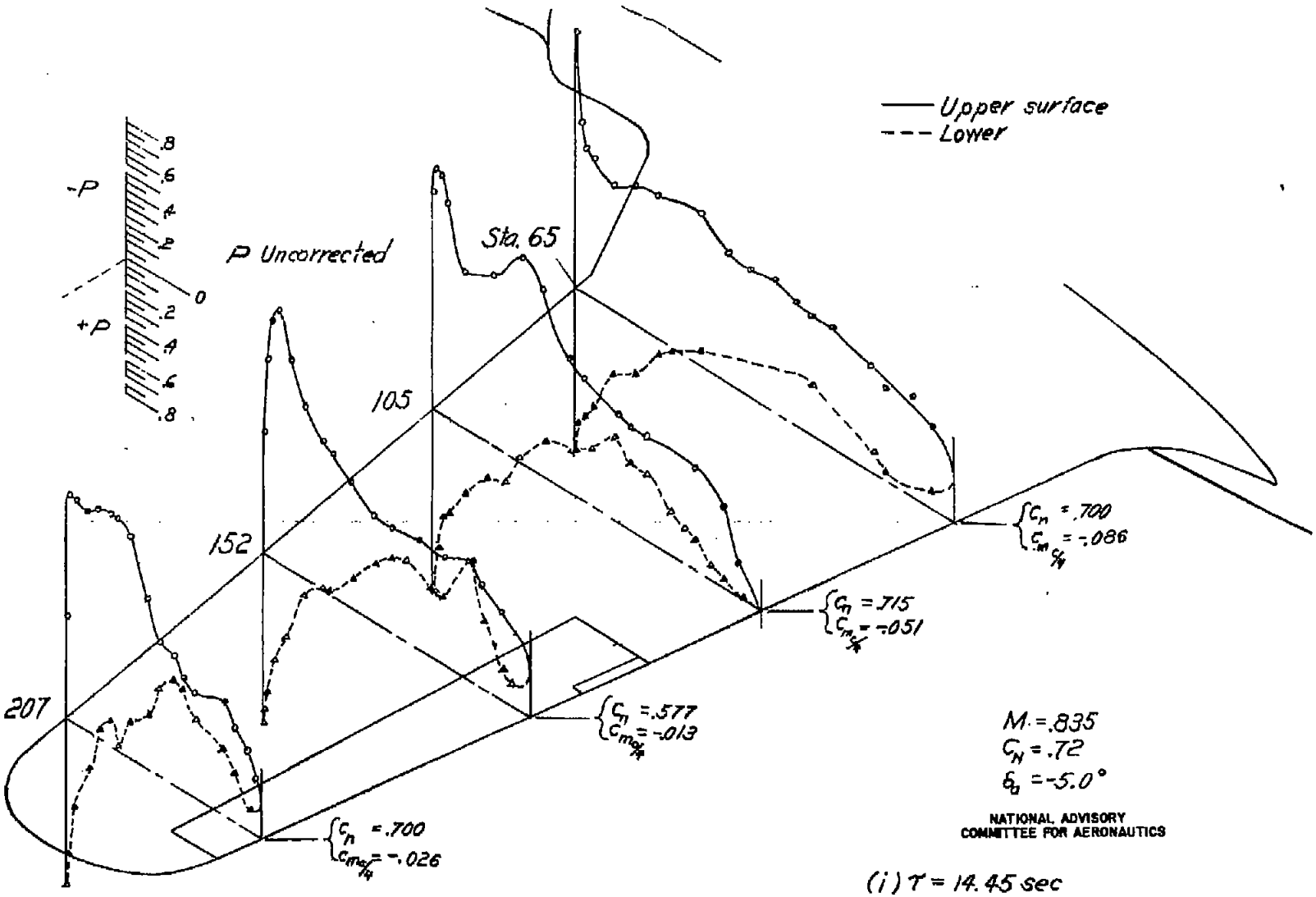

Figure 7. — Continued.

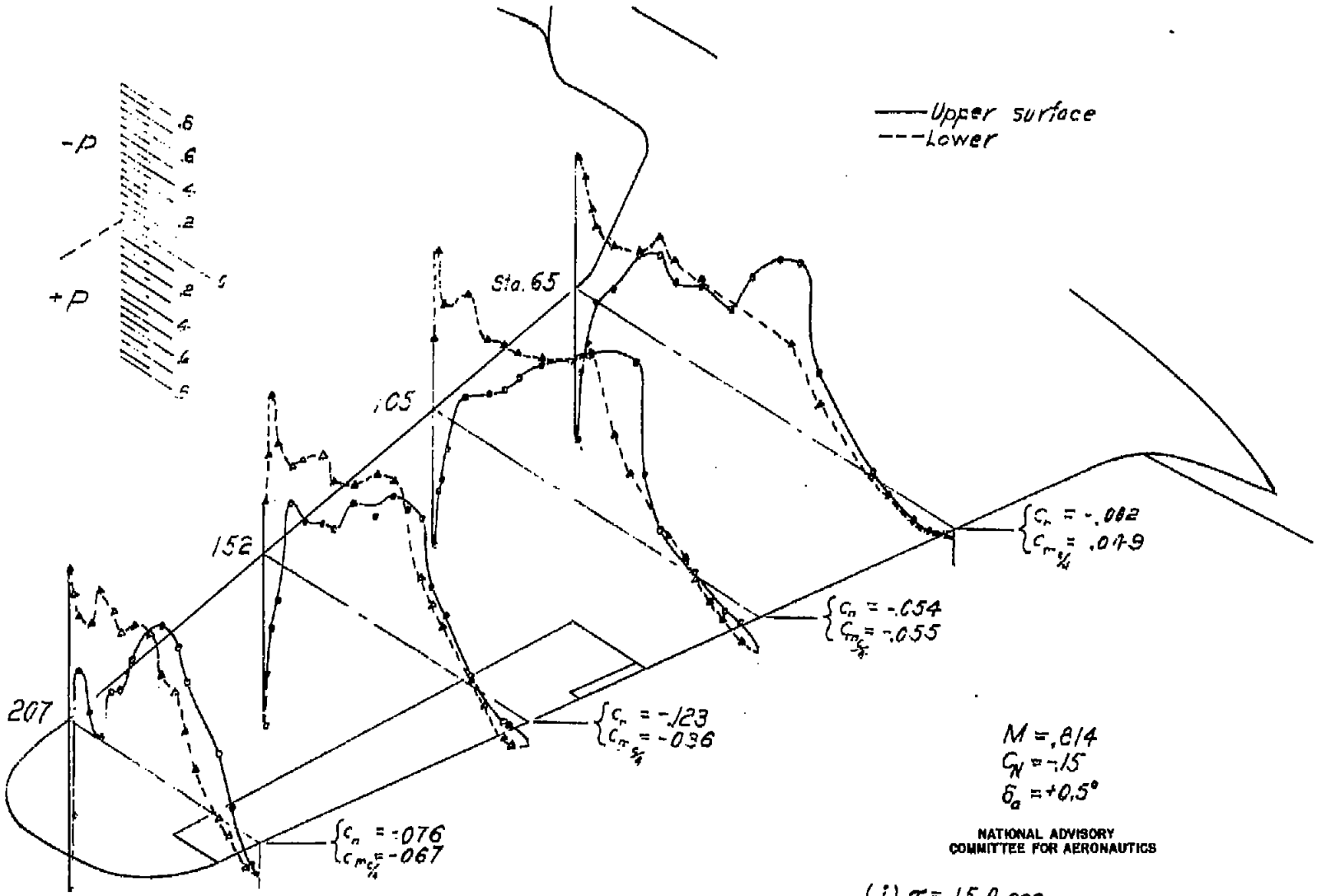

(j) T = 15.0 sec

Figure 7.— Concluded.

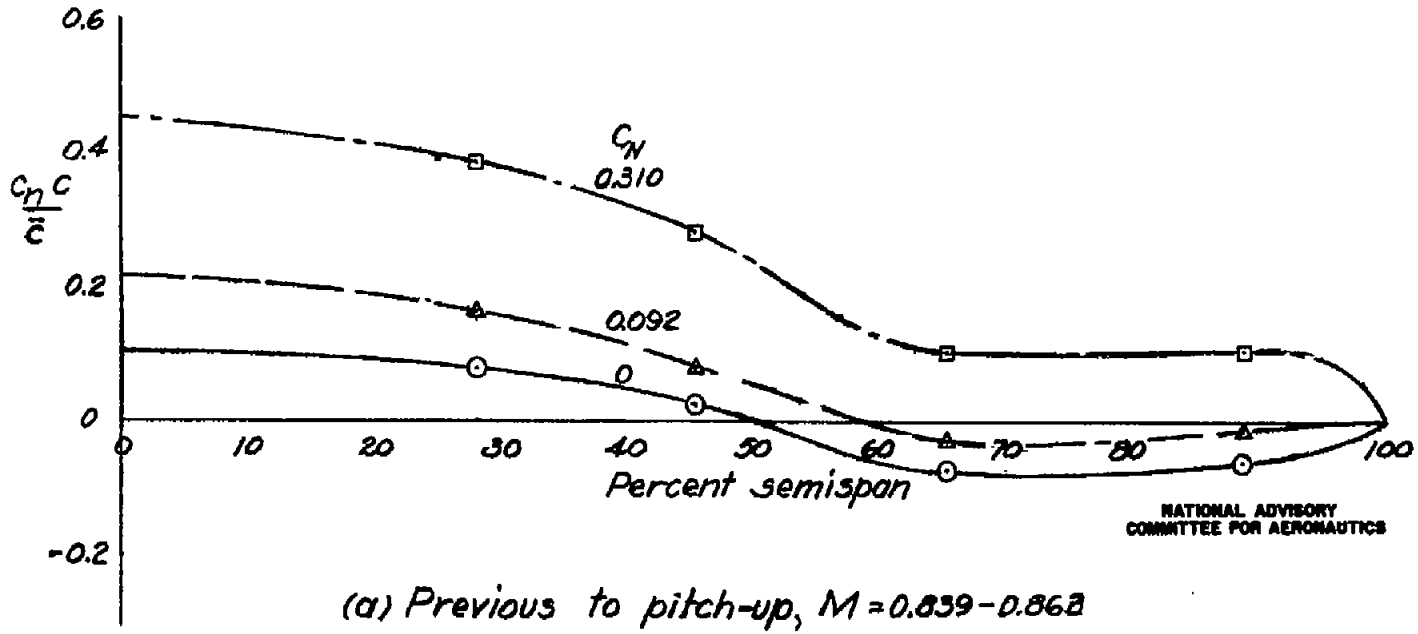

(a) Previous to pitch-up, $M = 0.839 - 0.868$

Figure 8.— Spanwise loading at various values of normal-force coefficient during dive recovery.

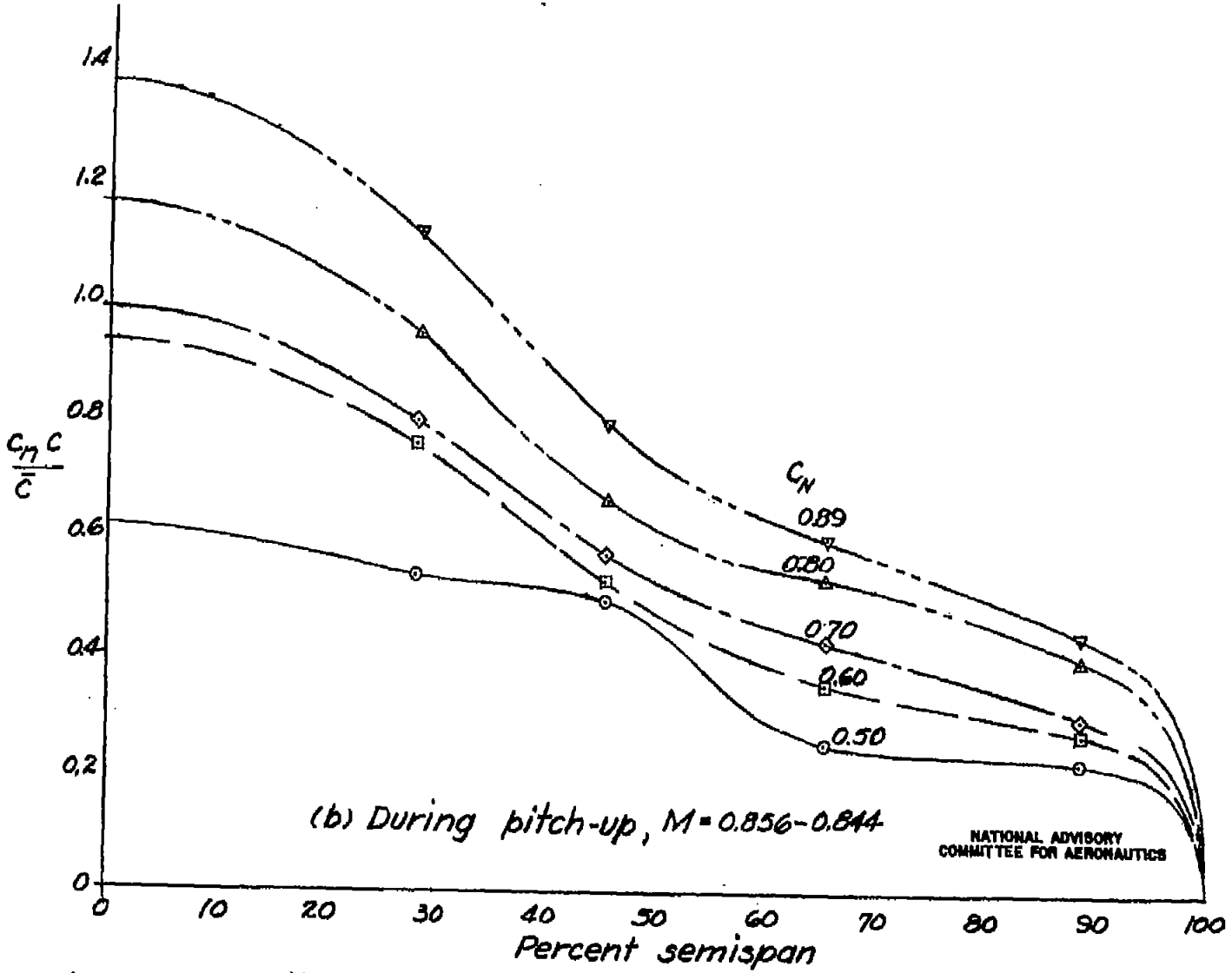

Figure 8.— continued.

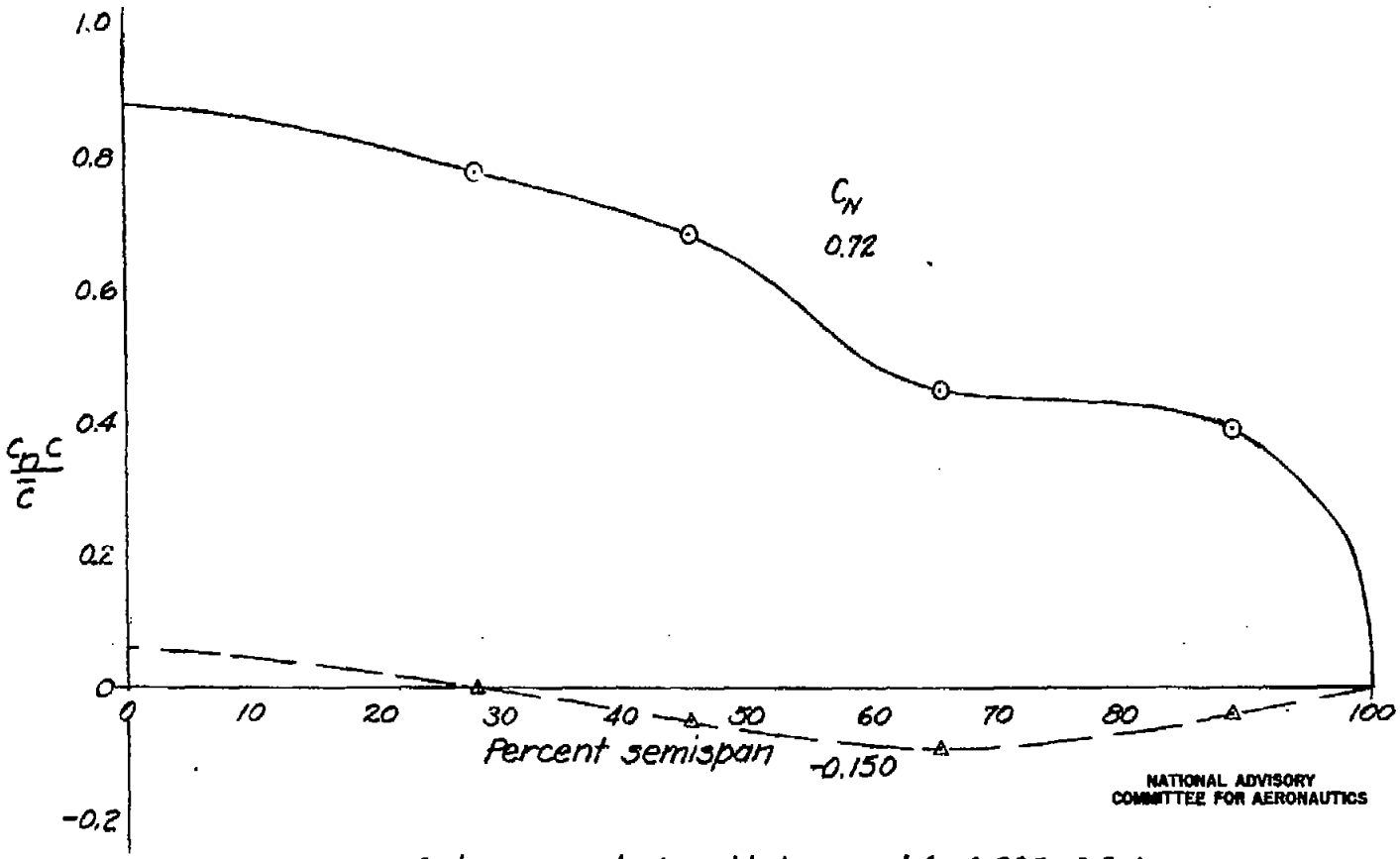

(c) Subsequent to pitch-up, $M = 0.835 - 0.814$

Figure 8.— concluded.

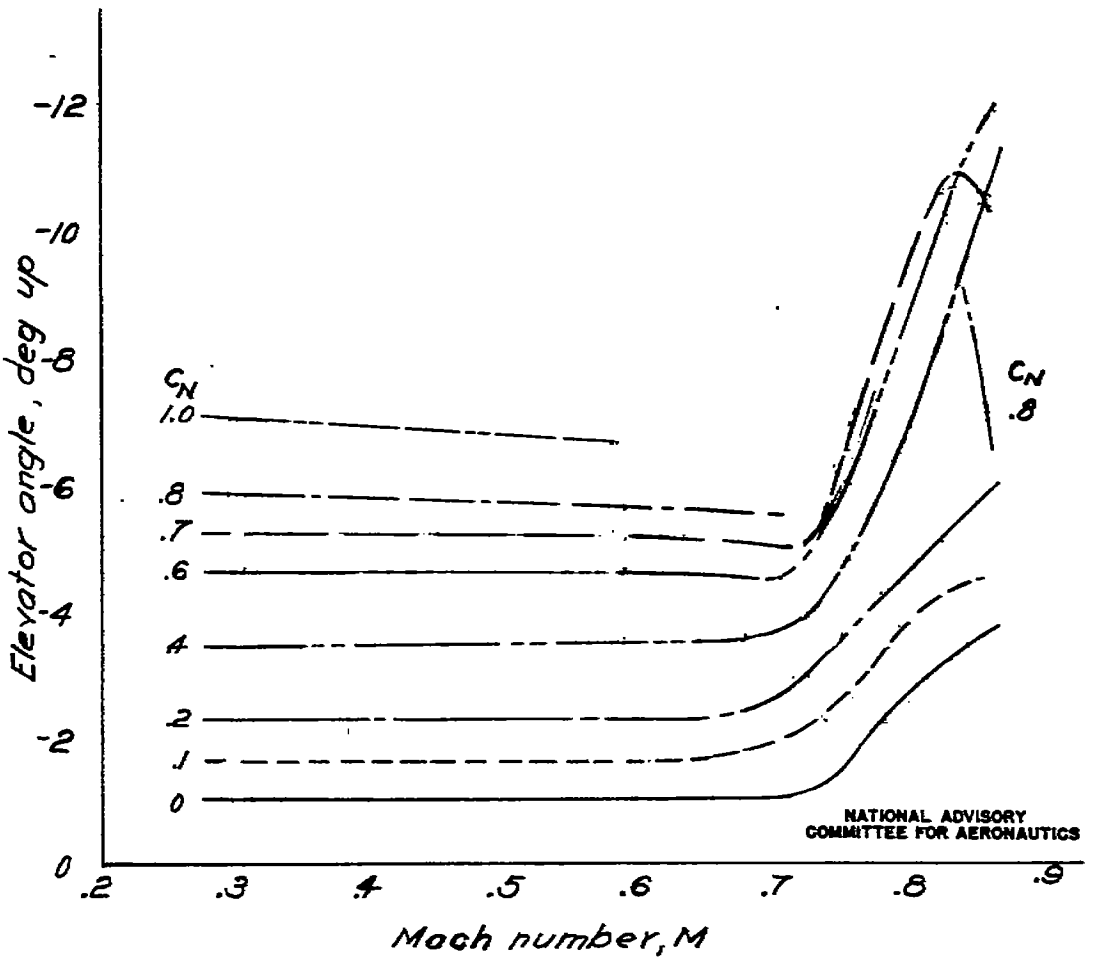

Figure 9.— Variation of elevator angle with Mach number for various values of airplane normal-force coefficient obtained from flight test.

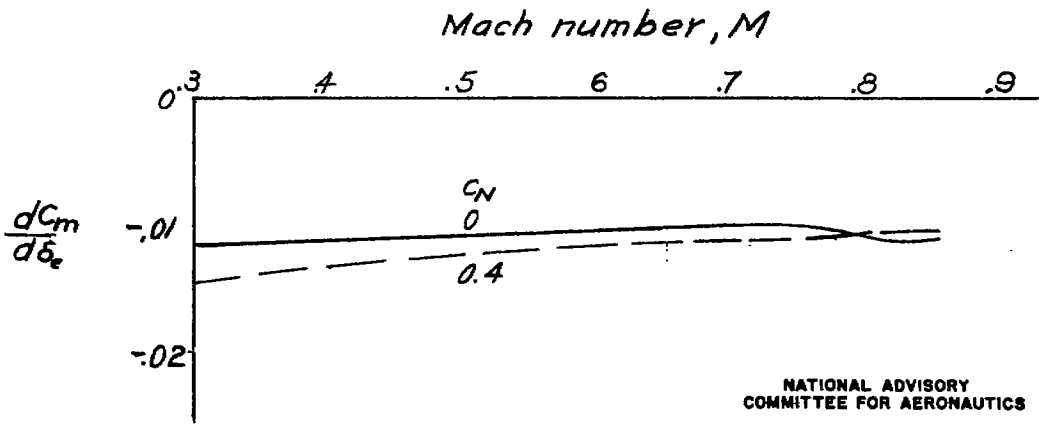

(a) Elevator effectiveness

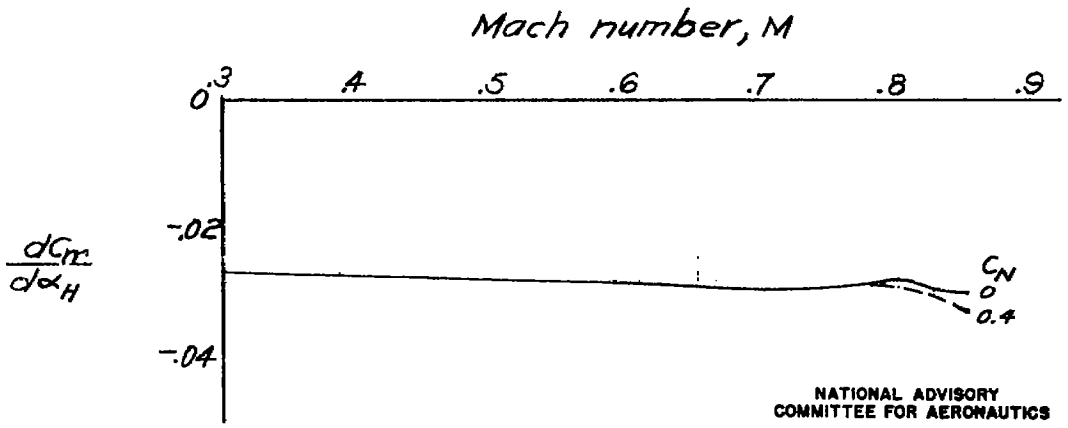

(b) Stabilizer effectiveness

Figure 10.— Horizontal-tail characteristics obtained in high-speed wind-tunnel tests of $\frac{1}{3}$-scale model of test airplane (ref. 2).

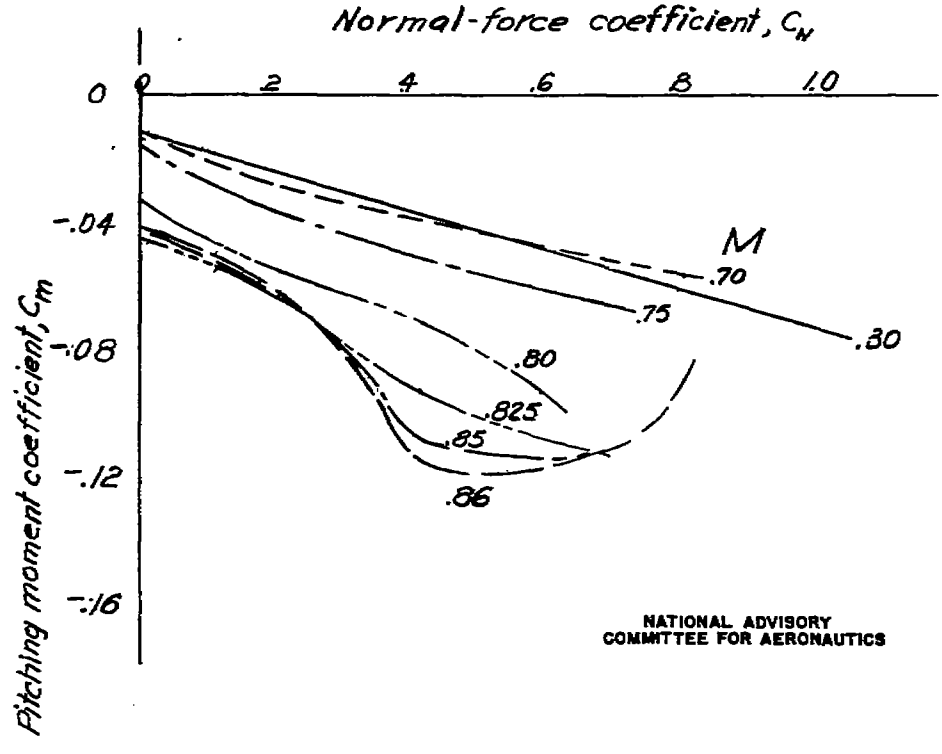

Figure 11.— Apparent longitudinal stability of test airplane.

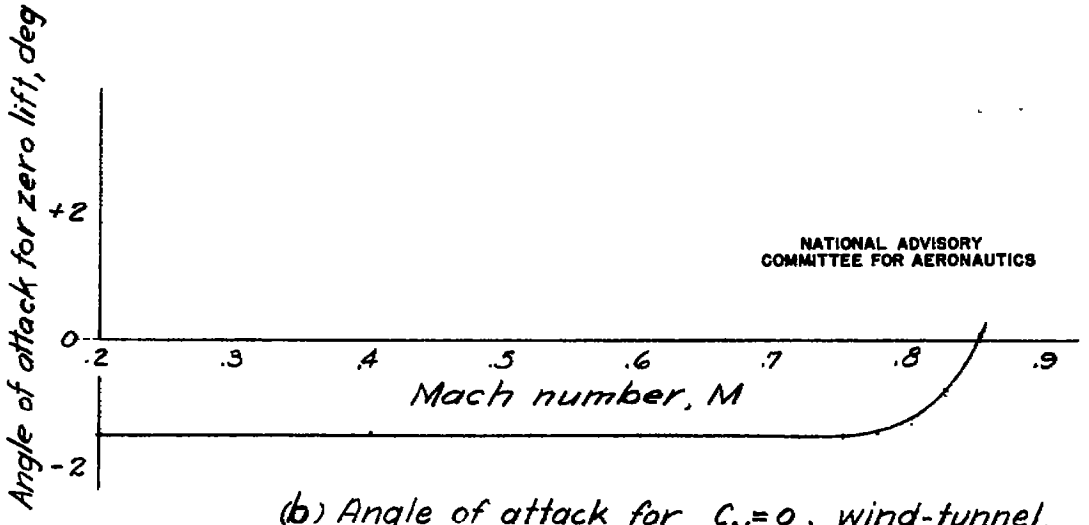

(b) Angle of attack for $C_N = 0$, wind-tunnel, (Ref. 2)

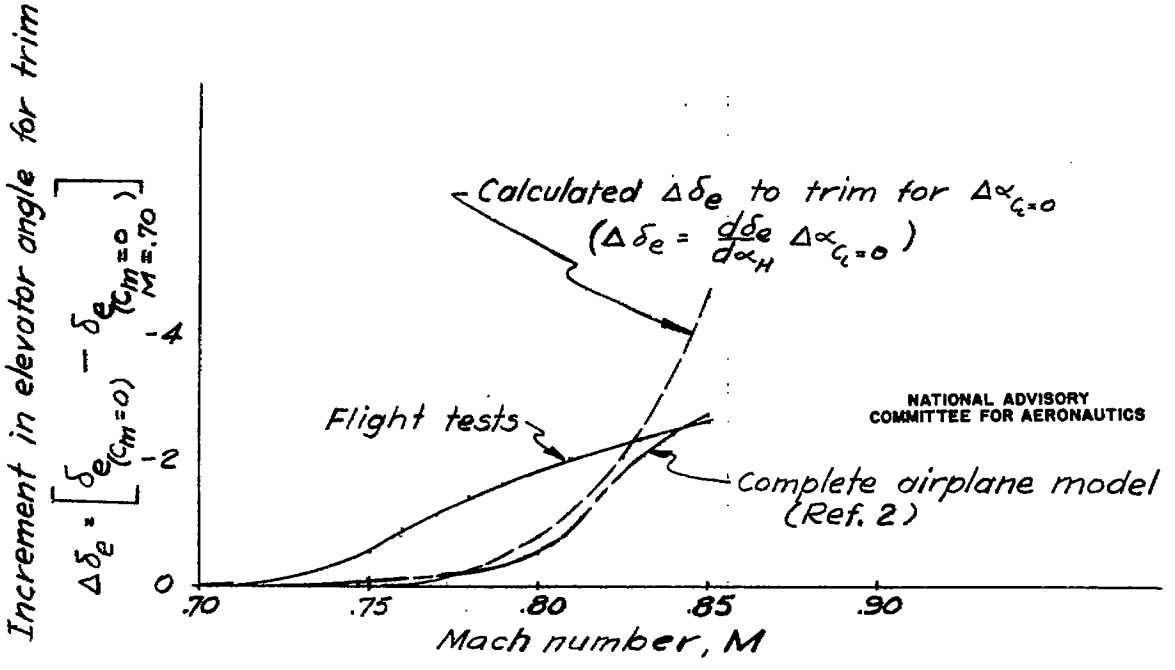

(a) Incremental elevator deflection.

Figure 12.— Variation with Mach number of incremental elevator deflection required for balance above $M = 0.70$ and angle for zero lift.

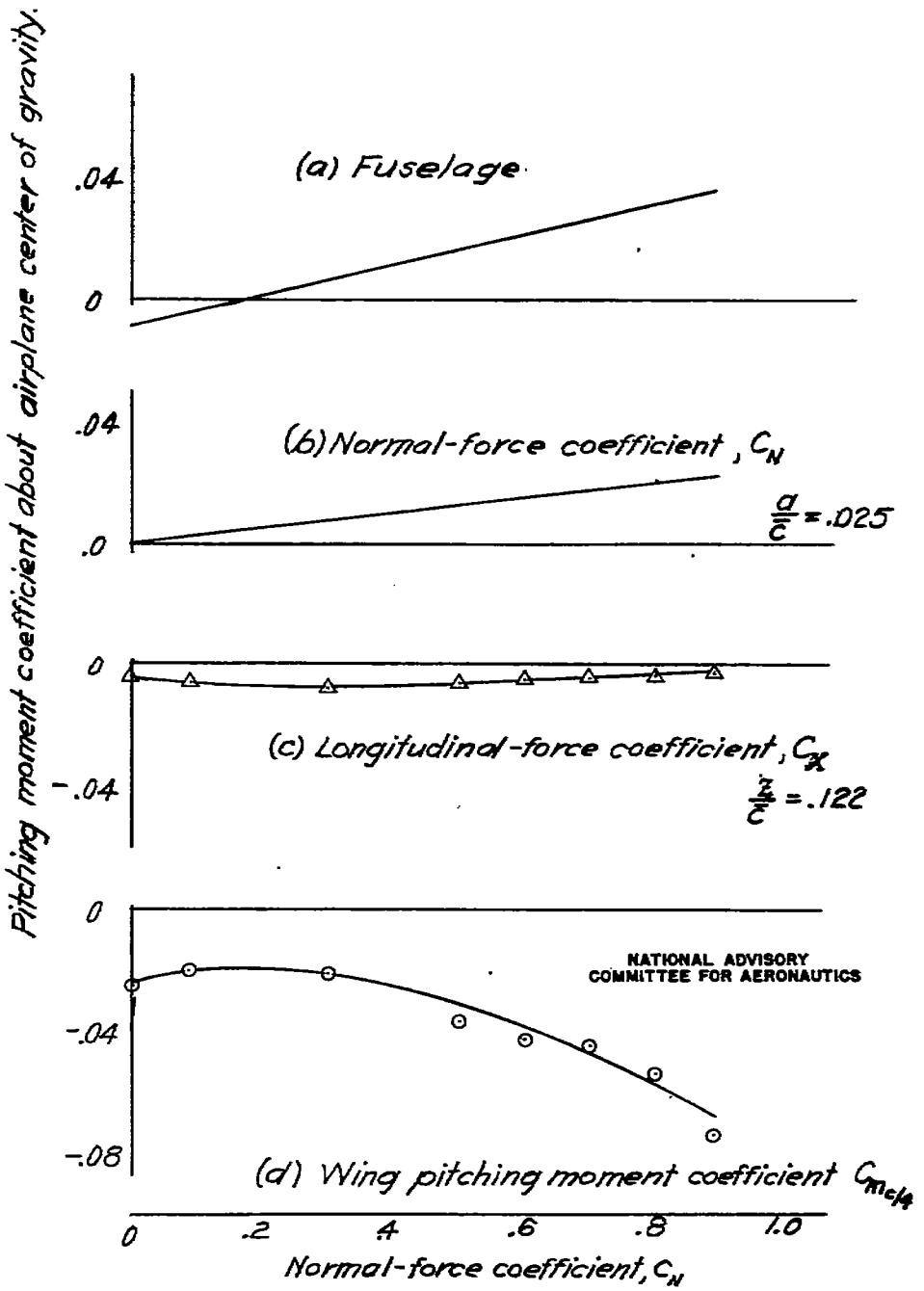

Figure 13.—Variation of the quantities affecting the airplane tail-off pitching-moment coefficient with normal-force coefficient during the dive.

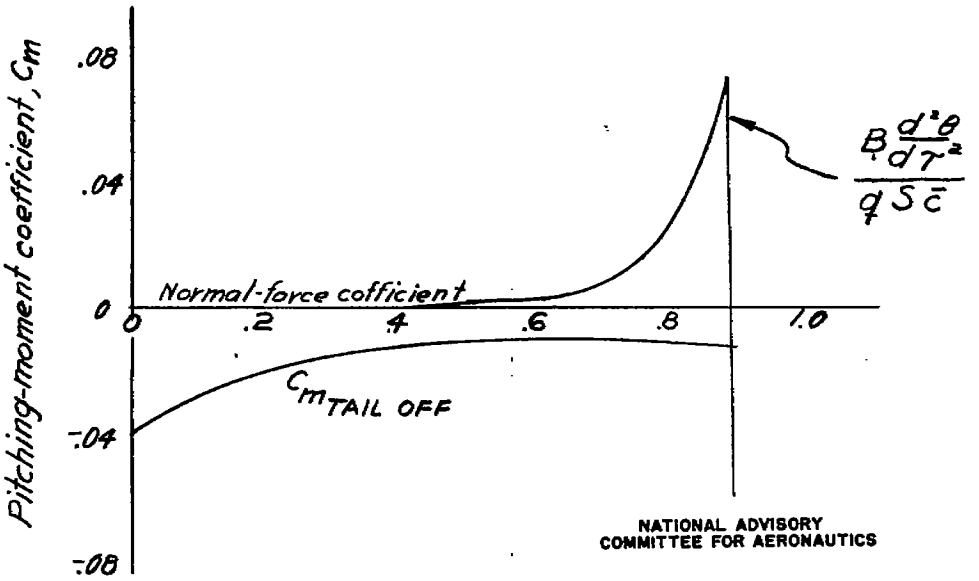

Figure 14.—Derived pitching-moment characteristics of the test airplane during the dive.

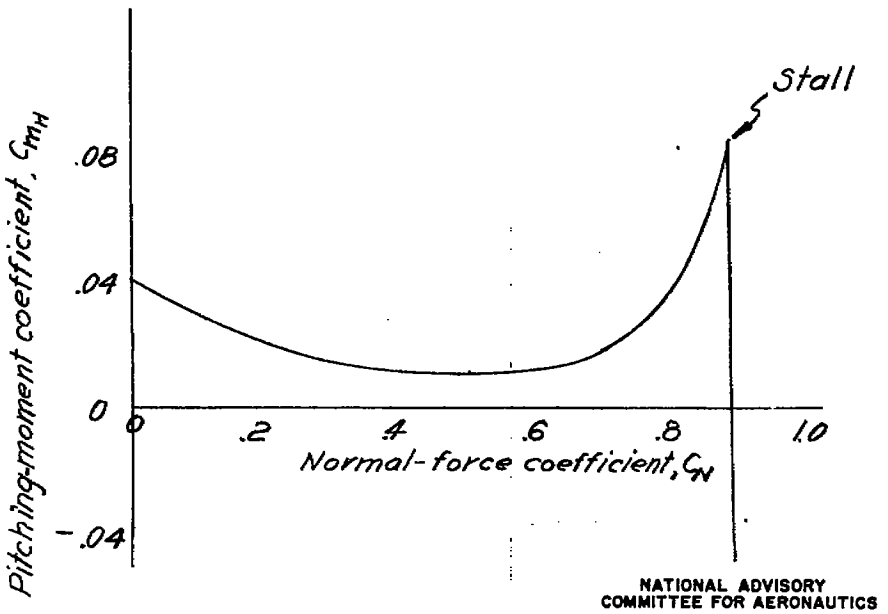

Figure 15.— Derived pitching-moment coefficient of the horizontal tail during the dive.

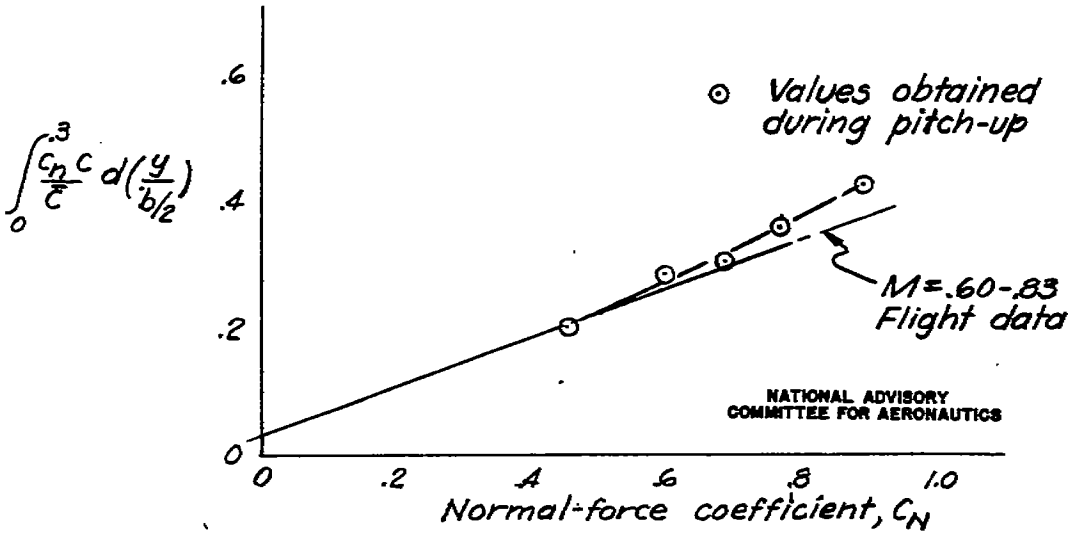

Figure 16.— Variation of wing load over center section with normal-force coefficient.

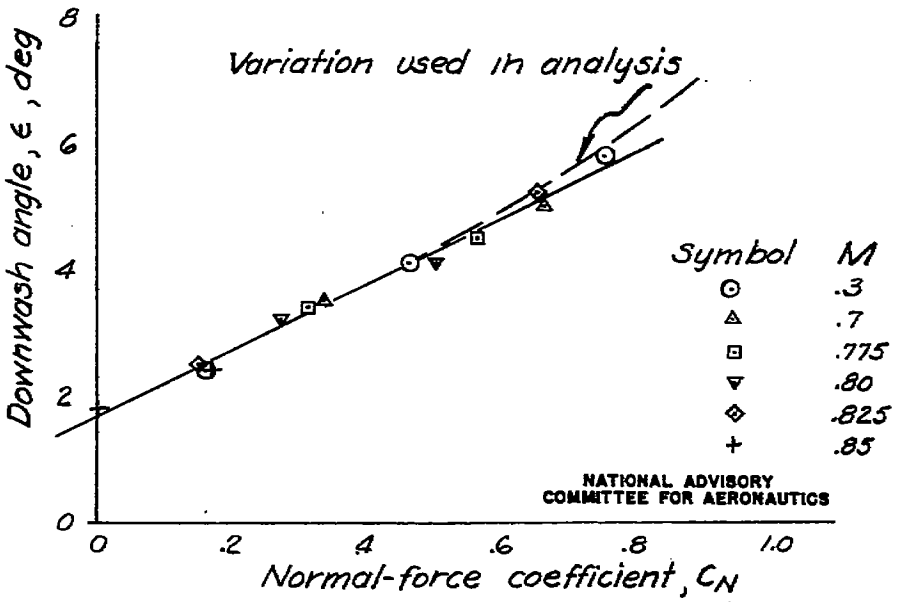

Figure 17.— Variation of downwash angle with normal-force coefficient from tests in the Ames 16 FT High-speed Wind Tunnel and corrected variation used in analysis.

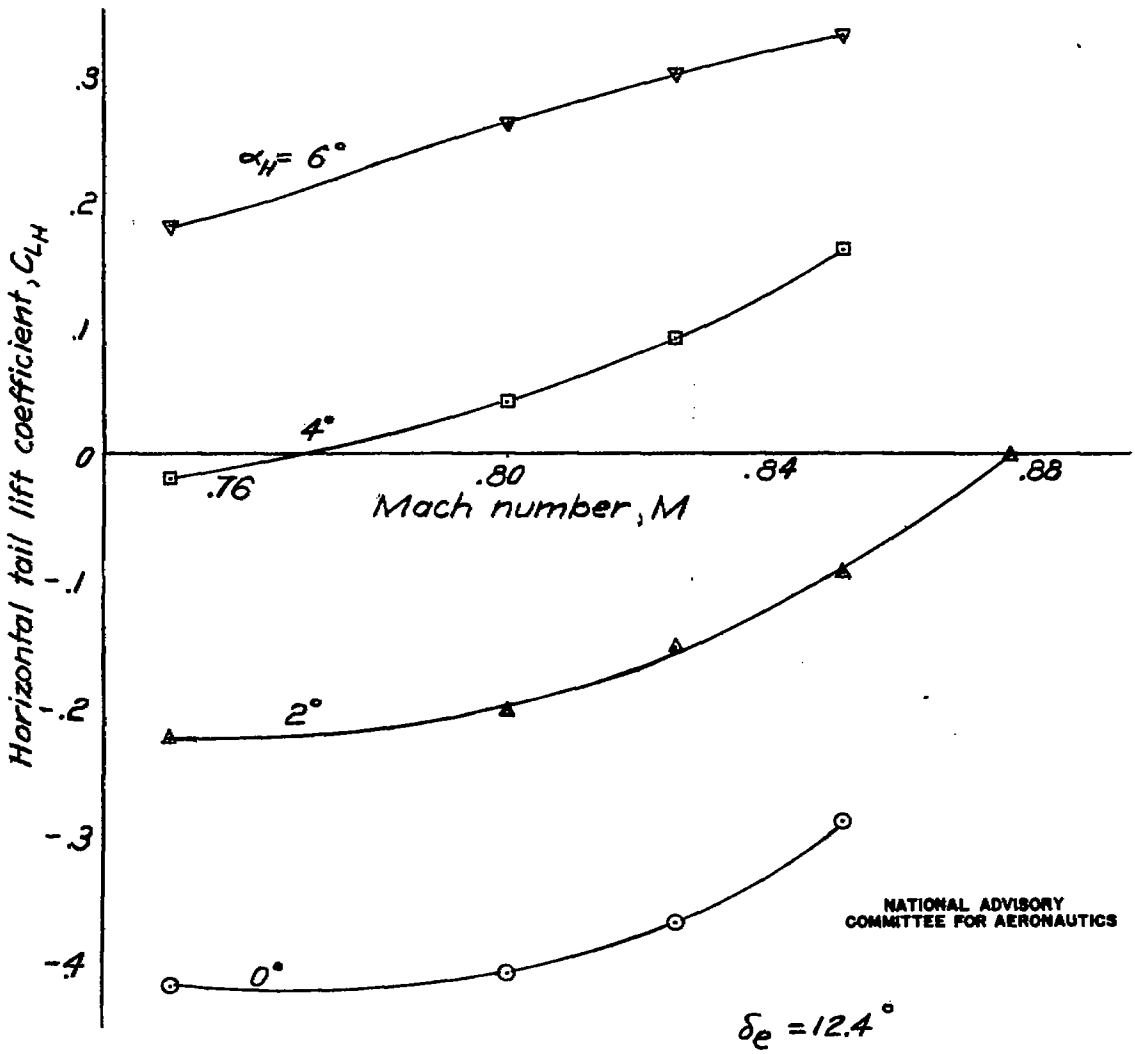

Figure 18.— Variation of the horizontal-tail lift coefficient with Mach number for constant values of tail angle of attack.

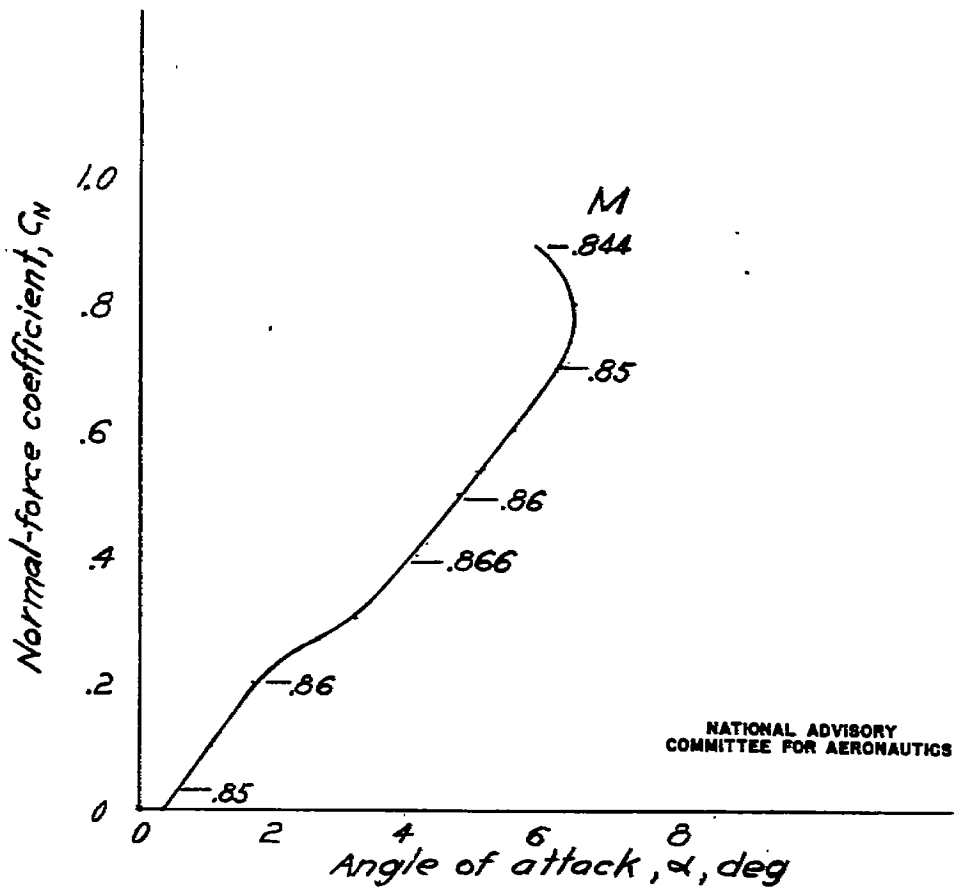

Figure 19.–Derived variation of normal-force coefficient with angle of attack required to produce the dive recovery.

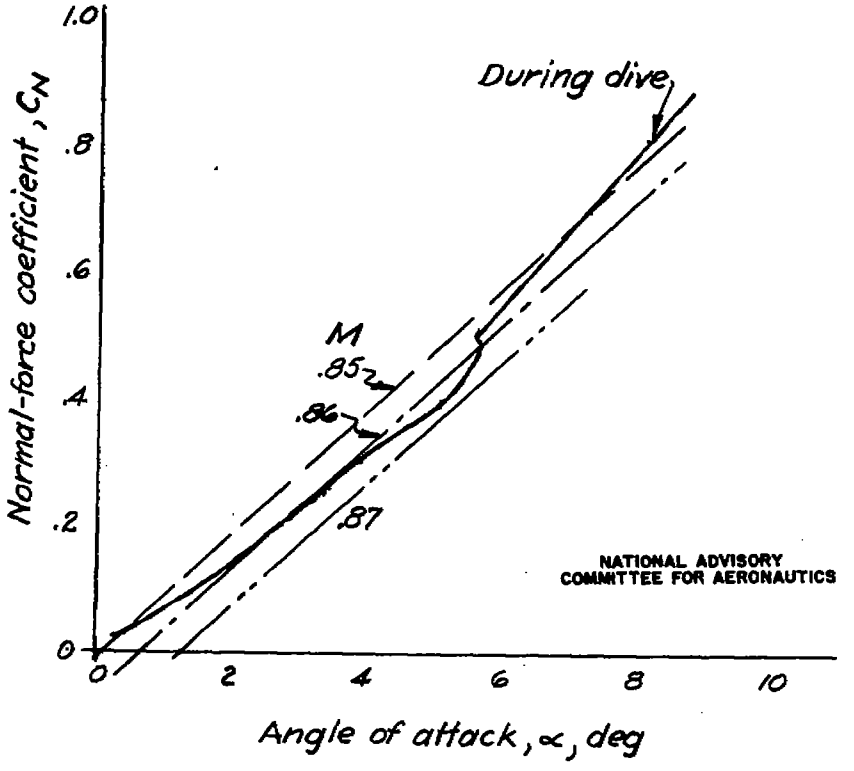

Figure 20.— Assumed variation of normal-force coefficient with angle of attack.

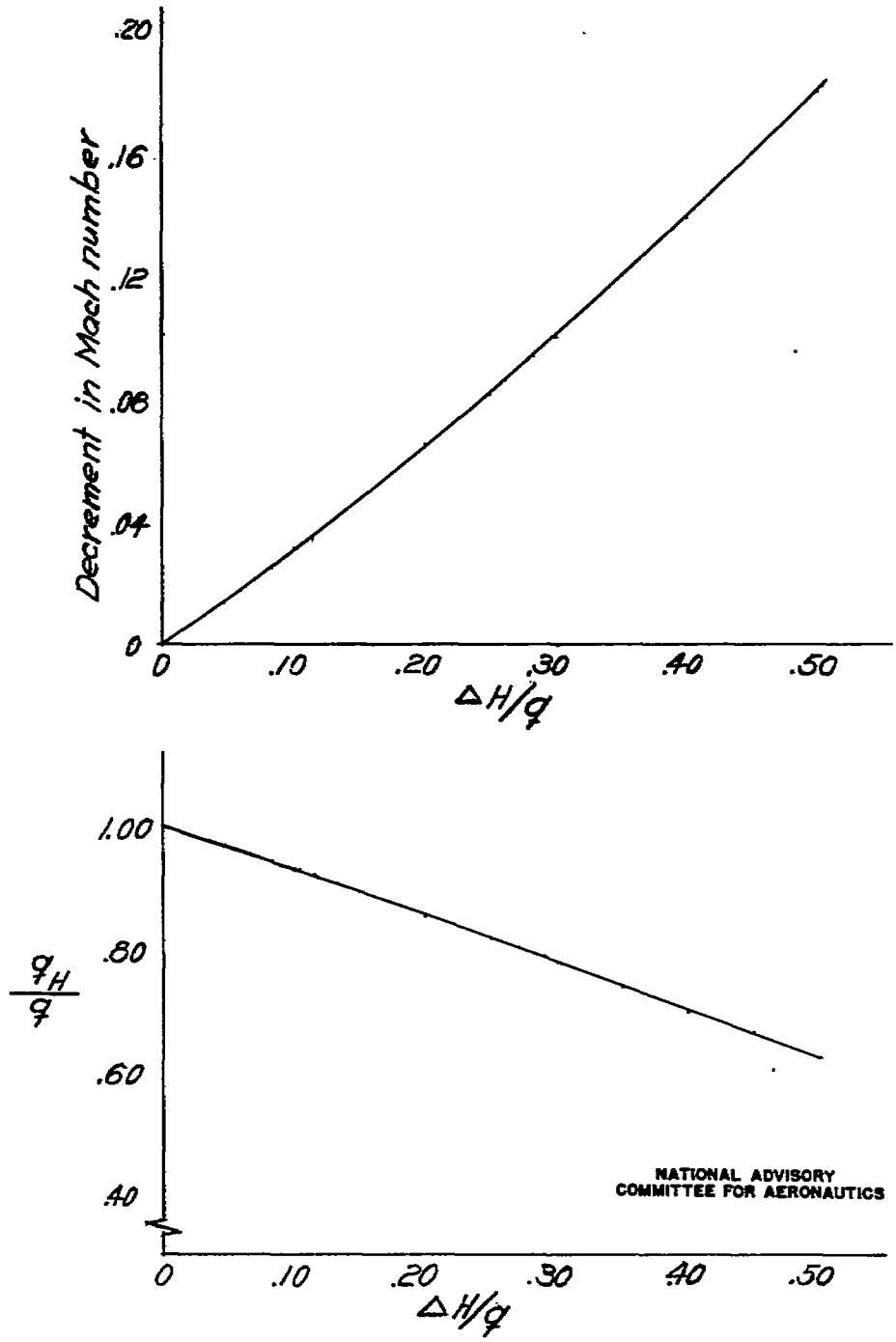

Figure 21.- Decrement in Mach number and variation of dynamic pressure due to a loss in total head for an initial Mach number of 0.85.

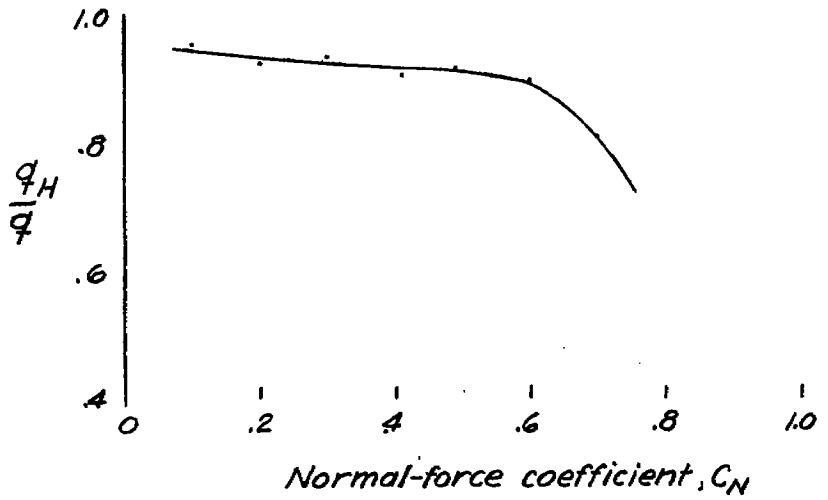

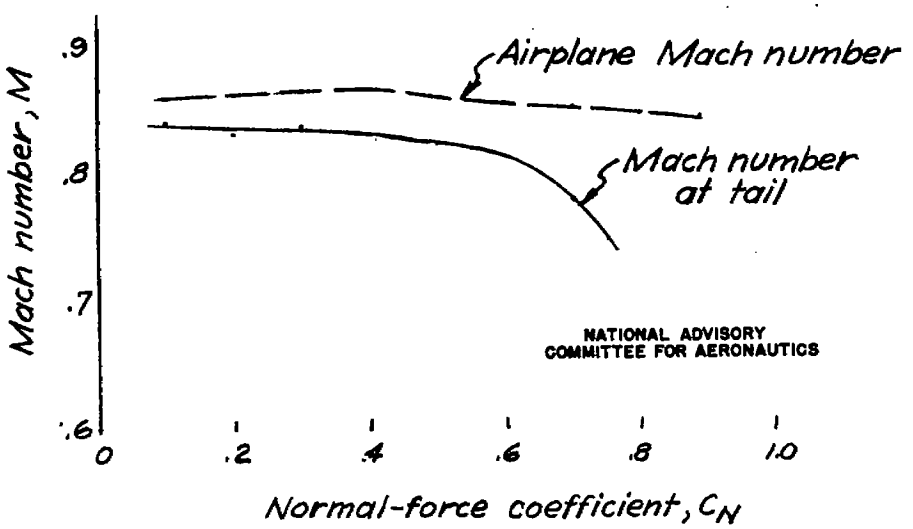

Figure 22.— Variation of dynamic pressure ratio and Mach number at the tail required to produce the dive recovery.

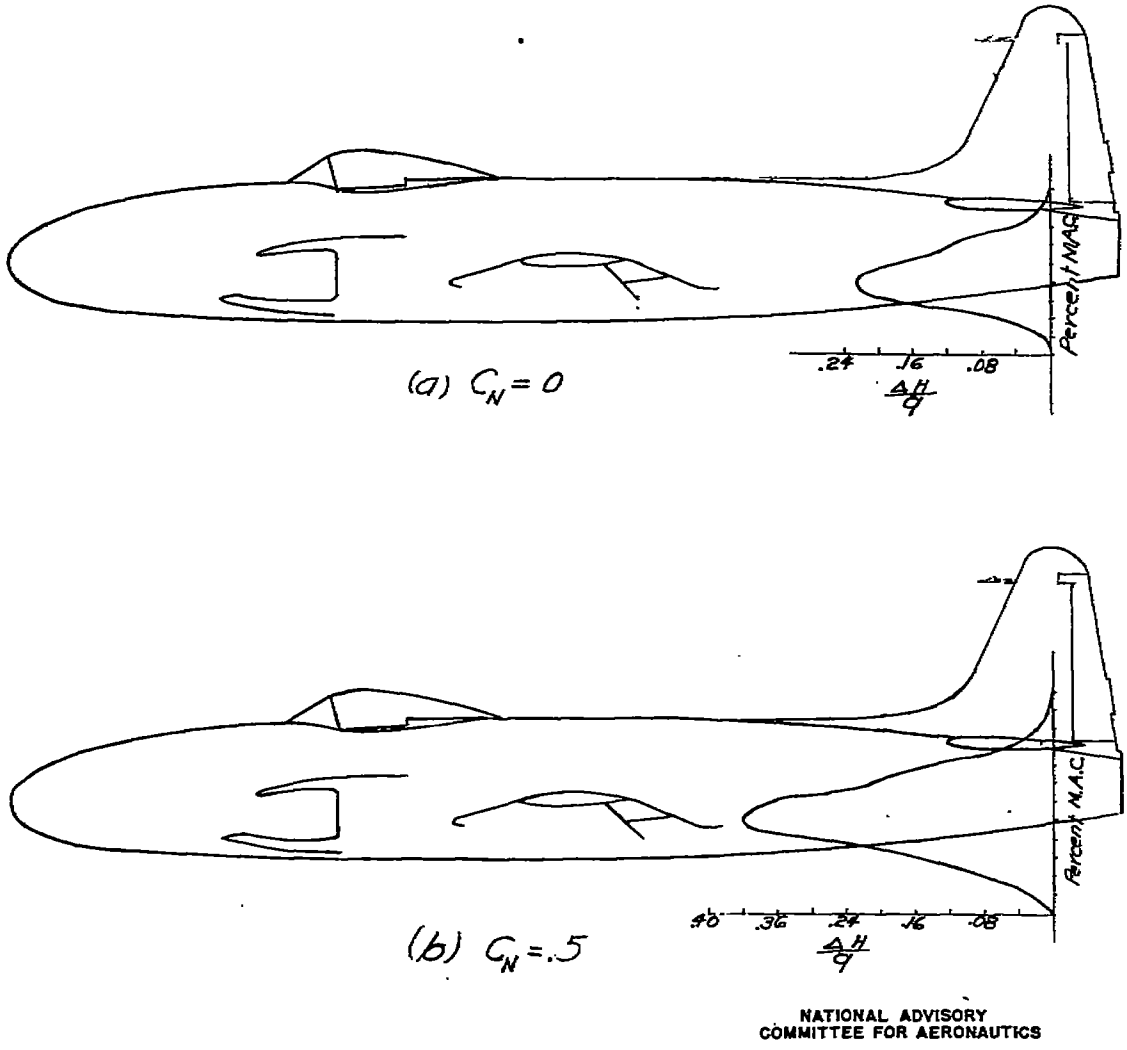

Figure 23.–Estimated wake conditions at the hinge line of the horizontal tail at approximately 0.85 Mach number.

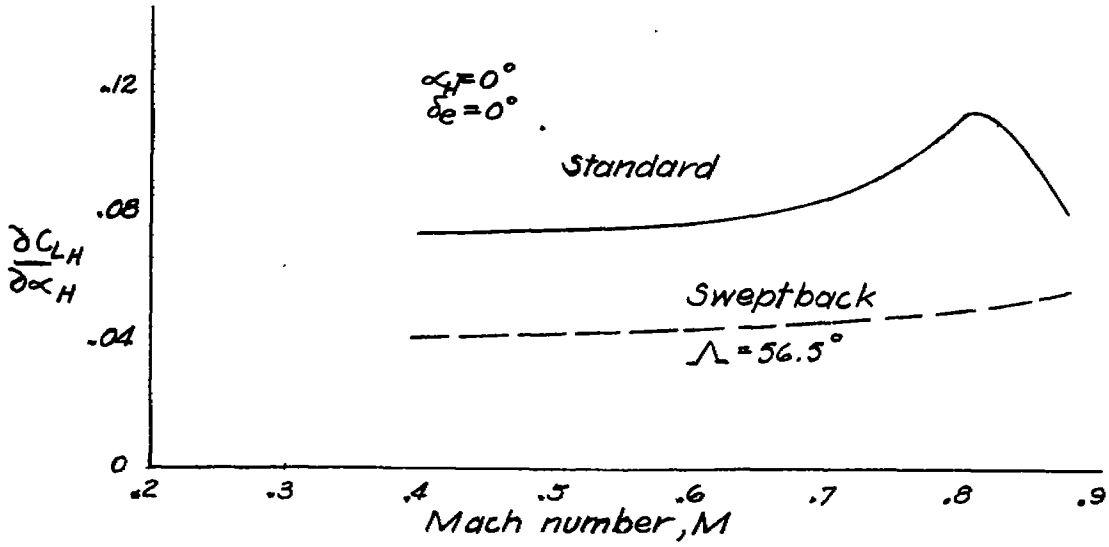

(a) Stabilizer effectiveness

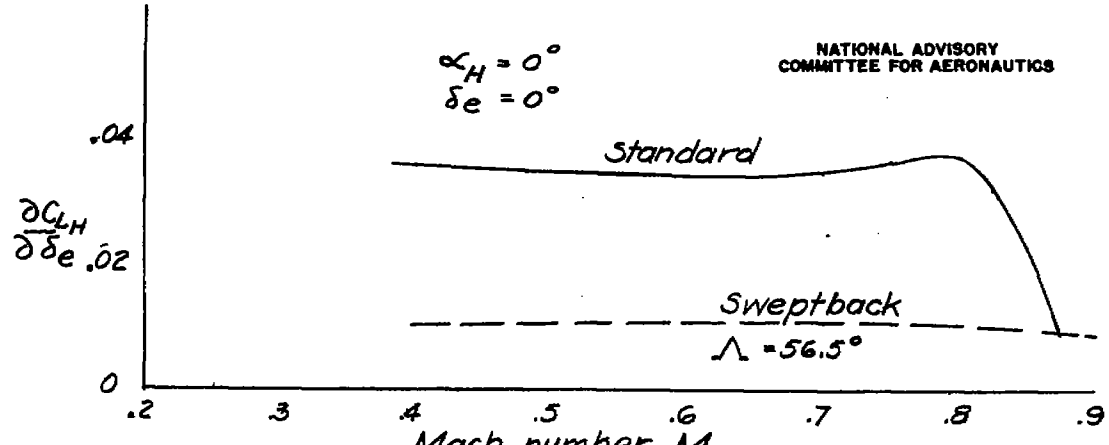

(b) Elevator effectiveness

Figure 24.— Horizontal-tail characteristics from tests of a 1/3-scale model in Ames 16 Ft. High-speed Wind Tunnel.